

# 1 **Neuronal circuits integrating visual motion information in *Drosophila***

2

3 Kazunori Shinomiya<sup>1\*,#a</sup>, Aljoscha Nern<sup>1</sup>, Ian A. Meinertzhagen<sup>1,2</sup>, Stephen M. Plaza<sup>1, #b</sup>, and  
4 Michael B. Reiser<sup>1\*</sup>

5

6 1: Janelia Research Campus, Howard Hughes Medical Institute, Ashburn, Virginia, United States

7 2: Department of Psychology and Neuroscience, Dalhousie University, Halifax, Nova Scotia, Canada

8 #a: Present address: Center for Computational Neuroscience, Flatiron Institute, Simons Foundation, New York, New  
9 York, United States

10 #b: Present address: Meta, Menlo Park, California, United States

11 \*: Corresponding authors: [kshinomiya@flatironinstitute.org](mailto:kshinomiya@flatironinstitute.org) (KS), [reiserm@janelia.hhmi.org](mailto:reiserm@janelia.hhmi.org) (MBR)

12

## 13 **Summary**

14

15 The detection of visual motion enables sophisticated animal navigation, and studies in flies have  
16 provided profound insights into the cellular and circuit basis of this neural computation. The  
17 fly's directionally selective T4 and T5 neurons respectively encode ON and OFF motion. Their  
18 axons terminate in one of four retinotopic layers in the lobula plate, where each layer encodes  
19 one of four cardinal directions of motion. While the input circuitry of the directionally selective  
20 neurons has been studied in detail, the synaptic connectivity of circuits integrating T4/T5 motion  
21 signals is largely unknown. Here we report a 3D electron microscopy reconstruction, wherein we  
22 comprehensively identified T4/T5's synaptic partners in the lobula plate, revealing a diverse set  
23 of new cell types and attributing new connectivity patterns to known cell types. Our  
24 reconstruction explains how the ON and OFF motion pathways converge. T4 and T5 cells that  
25 project to the same layer, connect to common synaptic partners symmetrically, that is with  
26 similar weights, and also comprise a core motif together with bilayer interneurons, detailing the  
27 circuit basis for computing motion opponency. We discovered pathways that likely encode new  
28 directions of motion by integrating vertical and horizontal motion signals from upstream T4/T5  
29 neurons. Finally, we identify substantial projections into the lobula, extending the known motion  
30 pathways and suggesting that directionally selective signals shape feature detection there. The  
31 circuits we describe enrich the anatomical basis for experimental and computational analyses of  
32 motion vision and bring us closer to understanding complete sensory-motor pathways.

## 33 Introduction

34

35 The *Drosophila melanogaster* visual system has been crucial for uncovering circuit mechanisms  
36 of many neural computations, such as detecting visual motion, looming, and color opponency<sup>1-8</sup>.  
37 Genetic driver lines enable functional studies of these computation<sup>9-13</sup>, often testing circuit  
38 hypotheses suggested by recent connectomes based on three-dimensional electron microscopy  
39 (3D-EM). The fly optic lobe has four major neuropils (lamina, medulla, lobula, and lobula plate;  
40 Figure 1A) that are characterized by columnar neurons connecting these structures, and striking  
41 layer patterns housing these connections. The diversity of optic lobe neuron types has been well  
42 documented using Golgi's and silver staining methods<sup>14,15</sup>, and in recent years, genetic driver  
43 lines for cell-type-specific expression and new tools for neuroanatomy<sup>11,16,17</sup>.

44

45 Small volume EM reconstructions have revealed the synaptic connectivity of many neurons in  
46 the lamina, medulla, and lobula<sup>18-23</sup>, with special attention to the columnar neurons of the motion  
47 processing pathway. Together with functional studies, these reconstructions have revealed the  
48 detailed neuronal circuitry and the likely mechanism(s) of motion detection by T4 and T5  
49 neurons. T4 are the ON directionally selective neurons. They encode the direction of motion,  
50 while none of their dendritic inputs (in medulla layer M10) do<sup>24</sup>. T5 are OFF directionally  
51 selective neurons that encode the direction of moving dark edges, by integrating inputs onto their  
52 dendrites in the first lobula layer (Lo1)<sup>22,25</sup>. Both cells have four distinct subtypes, a, b, c, and d.  
53 Each subtype projects axons to one of the four layers of the lobula plate (Figure 1B), where their  
54 terminals are retinotopically arranged<sup>8,14</sup>.

55

56 The lobula plate is the fourth neuropil in the optic lobe, and the evolutionary origin of this  
57 conserved neuropil has been hypothesized to relate to the origin of insect flight<sup>26</sup>. In Diptera  
58 (flies), the neuropil is best known for containing the dendrites of the 'giant' lobula plate  
59 tangential cells (LPTCs) that respond to specific patterns of visual motion<sup>15,27-30</sup>. The vertical  
60 system (VS) and horizontal system (HS) cells are the best studied LPTCs, and homologous  
61 neurons have been identified in both larger flies and *Drosophila*<sup>14,28</sup>. The arborization patterns of  
62 HS and VS cells in the *Drosophila* lobula plate were examined using the GAL4-UAS system and  
63 single cell labeling, confirming neuron morphology that closely resembles the corresponding

64 cells of larger flies<sup>31</sup>, and the electrophysiologically measured response properties of these cells  
65 to visual motion patterns match those of larger flies<sup>32,33</sup>.

66

67 Based on imaging T4/T5 responses in the lobula plate<sup>8</sup>, it is now understood that each layer  
68 integrates inputs corresponding to one cardinal direction of motion: front-to-back (Lop1), back-  
69 to-front (Lop2), upward (Lop3), and downward (Lop4). Anatomical and physiological data  
70 suggest a correlation between an LPTC's visual motion responses and its lobula plate layer  
71 pattern<sup>28,34</sup>. Further details of the lobula plate circuitry have not been thoroughly investigated,  
72 with the noteworthy exception of two bilayer lobula plate intrinsic (LPi) cells: LPi3-4 receive  
73 input in Lop3 and provide output to Lop4, while LPi4-3 sends signals from Lop4 to Lop3<sup>14,35,36</sup>.  
74 These LPi cells have been shown to inhibit their target LPTCs in response to 'opponent' motion.  
75 This sharpens the flow-field selectivity of the tangential cells, in a computation termed 'motion  
76 opponency'<sup>35</sup>. Functional studies<sup>3,35,37</sup> suggest that the site of action is the integration of  
77 excitatory, cholinergic T4 and T5 input together with inhibitory, glutamatergic LPi inputs by  
78 LPTCs, but the synaptic connectivity proposed by this parsimonious circuit hypothesis has not  
79 been verified.

80

81 The lobula plate also houses processes of columnar neuron types other than T4 and T5, including  
82 optic lobe-intrinsic neurons, such as Y, TmY (transmedulla Y), and Tlp (trans lobula plate) cells,  
83 which connect different optic lobe neuropils, and the LPC (lobula plate columnar), LLPC  
84 (lobula-lobula plate columnar), and LPLC (lobula plate-lobula columnar) cells, which are visual  
85 projection neurons (VPNs) into the central brain<sup>3,14,38-44</sup>. Detailed connectivity information for  
86 the principal neurons of the lobula plate, especially T4 and T5, LPTCs, LPis, and other columnar  
87 neurons, is largely unknown, and represents the last piece of the puzzle for the anatomical  
88 description of the primary motion information-processing circuit in the optic lobe. To close this  
89 gap, we reconstructed the neurons downstream of T4 and T5 in the lobula plate using an optic  
90 lobe dataset imaged with focused-ion beam-aided scanning electron microscopy (FIB-SEM)<sup>22,45</sup>.  
91 We exhaustively identified and cataloged T4 and T5 synaptic partners, and investigated complete  
92 synaptic profiles of the LPi cells that connect two layers of the lobula plate, as well as the HS  
93 and VS cells. In the process, we identified new cell types and attributed new connectivity

94 patterns to known cell types, resolving several open questions about lobula plate connectivity,  
95 while also establishing many new neurons as important components of the motion pathway.

96

## 97 **Results**

98

### 99 **EM reconstruction of the synaptic partners of T4 and T5 cells in the lobula plate**

100 Our FIB-SEM data volume<sup>22,45</sup> includes large parts of the lamina, medulla, lobula, and lobula  
101 plate (Figure 1A), covering regions corresponding to the eye's equator, but not including the  
102 neuropils serving dorsal and ventral eye regions. Importantly this volume contains many  
103 connected neurons, corresponding to common retinotopic coordinates, enabling circuit  
104 reconstruction across these neuropils. Medulla neurons, including Mi1, Tm1, and Tm2, relay  
105 signals from lamina cells to T4, in M10, and T5, in Lo1 (Figure 1A)<sup>22</sup>. The four subtypes of T4  
106 and T5 send outputs to one of the four LOP layers (defined to encompass the terminals of groups  
107 of T4 and T5 cells, see Methods), where they synapse with other optic lobe interneurons and  
108 VPNs leading to the central brain (Figure 1B,C).

109

### 110 **Connectivity of the seed T4 and T5 cells in the lobula plate**

111 We reconstructed and then identified many neurons in the FIB-SEM volume, focusing on T4 and  
112 T5 cells and their targets. 277 T4s (66 T4a, 69 T4b, 74 T4c, 68 T4d) and 277 T5s (68 T5a, 74  
113 T5b, 71 T5c, 60 T5d) were identified and at least partially reconstructed. Five cells of each  
114 subtype from a retinotopically overlapping region near the volume center were completely  
115 traced<sup>22</sup>. In the prior study, we detailed the dendritic inputs of these neurons, and here we  
116 describe the connectivity of these same 40 cells in the lobula plate. All computationally predicted  
117 synapses (see Methods) of these cells were proofread to identify their pre- and post-synaptic  
118 partners.

119

120 The connectivity of the inputs and outputs of the representative T4 and T5 cells in the lobula  
121 plate is summarized in Figure 2A, including all neurons connected with  $\geq 5$  synapses to any of  
122 the seed T4 or T5 cell (detailed connectivity data in File S1). We found 56 putative connected  
123 neuron types (mean of  $\geq 5$  synapses with any T4 or T5), including unidentified fragments (Figure  
124 2A; shown in gray). 43 of these (77%) communicate with the same subtype of T4 and T5 within

125 a single layer, resulting in a connectivity diagram that is largely comprised of four clusters, each  
126 corresponding to synapses within one lobula plate layer. One noteworthy exception is LPLC2,  
127 which is the only neuron we identified that receives inputs from all four T4 and all four T5  
128 subtypes, corroborating the observations of a previous study that showed this cell type integrates  
129 spatially patterned inputs to selectively encode visual looming<sup>3</sup>.

130

131 How are the ON and OFF pathways integrated by targets in the lobula plate? In nearly every  
132 case, neurons that are strongly connected to T4/T5 have approximately symmetric inputs from  
133 T4 and T5, with a slight bias for T5 (pooled across all downstream neurons: 45.4% T4 vs. 54.6%  
134 T5), indicating that no major targets selectively integrate from only T4 or T5 (Figure 2B). This  
135 balanced integration of ON and OFF pathways suggests that any lobula plate neurons that  
136 primarily integrate inputs from T4 and T5 should not exhibit strongly asymmetric responses to  
137 bright vs. dark moving edges. However, some neurons may show differential sensitivity to dark  
138 or bright objects from other inputs. For example, LPLC2 responds strongly to dark looming  
139 stimuli and only weakly to bright looming<sup>3</sup>, despite substantial inputs from all T4/T5 subtypes  
140 (Figure 2B).

141

142 In mapping computational models onto the anatomy of the motion pathway, the T4/T5 axon  
143 terminals are treated as purely output structures<sup>35</sup>. We find that the axon terminals of T4 and T5  
144 are primarily sites of synaptic output, but have some inputs: 87% of T4's and 88% of T5's lobula  
145 plate synapses are presynaptic (T4: 1765.2 pre/cell, 270.0 post/cell; T5: 2125.4 pre/cell, 295.4  
146 post/cell). There are relatively small numbers of T4-T4, T5-T5, and T4-T5 connections within  
147 each layer. These occur between neighboring axon terminals, and each inter-terminal connection  
148 is typically  $\leq 3$  synapses. The number of pre- and postsynaptic sites per T4 and T5 varies by layer  
149 and individual neurons, but roughly follows a monotonic relationship; neurons with more output  
150 synapses tend to have more inputs (Figure 2C). For example, T4a and T5a neurons had more pre-  
151 and postsynapses than the other subtypes, due to strong connections with Lop1 neurons (Figure  
152 2A, File S1).

153

154 T4 and T5 cells provide strong inputs to a diverse set of VPNS, of which many are large  
155 tangential cells (identified cells named and indicated in green; Figure 2A). We focus on the

156 connectivity of the well-known HS and VS cells<sup>28,31</sup> in Figure 3. Small-field VPN types (LPC,  
157 LLPC, and LPLC cells)<sup>38,40,43,44</sup> are also found with substantial T4/T5 inputs in each layer. The  
158 morphology of many connected VPNs is shown in Figure 5. T4 and T5 cells in each layer  
159 provide strong inputs to four types of bilayer LPi cells, further explored in Figure 4. In addition  
160 to these cells, we identified many connections between T4/T5 neurons and other intrinsic optic  
161 lobe neurons, such as the TmY, Y, and Tlp cells (morphology shown in Figure 6) that  
162 interconnect different neuropils. For most newly described optic lobe intrinsic cell types, we  
163 provide light microscopy (LM) images as additional validation (Figures S1, S2). We summarize  
164 the core connectivity motifs at this output stage of the visual motion pathway in Figure 7.

165

### 166 **Synaptic connections of the Horizontal System (HS) and Vertical System (VS) lobula plate** 167 **tangential cells**

168 The HS and VS cells are prominent LPTCs whose response properties have been extensively  
169 studied<sup>31-33,46,47</sup>. They represent major T4/T5 targets in their respective layers (Figure 2A). In  
170 Lop1, T4a and T5a provide strong inputs to the HS cells, with a mean of 44.6 synapses from  
171 each T4a and 53.4 synapses from each T5a (File S1). Each lobula plate houses 3 HS cells, HSN,  
172 HSE, and HSS (north, equatorial, and south) cells, which respectively cover the dorsal, middle,  
173 and ventral parts of the visual field<sup>31</sup>. In our imaged volume, we find identifiable fragments of all  
174 three cells (Figures 3A,B). The dendrites of these cells are almost purely postsynaptic. Based on  
175 the computational predictions, HSN, HSE, and HSS respectively had 6151, 4514, and 2066  
176 postsynaptic densities (PSDs), and 7, 2, and 3 presynaptic T-bars. Most inputs to HS cells are  
177 from T4a and T5a (Figure 3F).

178

179 In Lop4, the VS cells receive a large portion of T4d and T5d's synaptic outputs (Figure 2A,B).  
180 We identified 10 VS or VS-like cells in Lop4 (Figure 3C, D). This number exceeds the expected  
181 count of VS cells in *Drosophila* based on earlier genetic labeling studies<sup>31</sup>, but is consistent with  
182 the number in larger flies<sup>30,48,49</sup> and a recent reconstruction in *Drosophila*<sup>34</sup>. These 10 cells have  
183 many common features: primary dendritic processes in Lop4, processes that are predominantly  
184 postsynaptic (typically >95% of total synapses), and simple connectivity profiles, with ~90% of  
185 inputs supplied by only three cell types (T4d, T5d, and LPi3-4; Figure 3F and Movie S1).  
186 Among the 10 VS and VS-like cells, four cells also have dendritic branches in Lop2 (Figure 3D);

187 some cells could feature branching in other layers outside of the volume). VS cells with dendritic  
188 arbors outside Lop4 have been previously described<sup>34,50</sup>. Boergens and colleagues identified six  
189 VS and three VS-like cells in their dataset<sup>34</sup>, of which eight had branches outside of Lop4.  
190 Integrating directionally selective inputs in other layers is expected to shape the flow-field  
191 selectivity of these neurons to incorporate regional horizontal motion that accompanies body and  
192 head rotation around certain axes<sup>47,50,51</sup>.

193  
194 The HS and VS cells are almost purely postsynaptic in the lobula plate. This connectivity from a  
195 very small set of cell types outlines a minimal number of circuit elements that could participate  
196 in the nonlinear summation of dendritic inputs by the HS and VS cells<sup>52</sup>. To quantify the input  
197 connectivity of these large neurons, we selected small ( $\leq 300$  PSDs) branches of HS cells (one  
198 each from HSN and HSS) and VS cells (two Lop4 branches and one Lop2 branch; each from  
199 different cells) and proofread all synaptic sites. An HS branch and a Lop4 VS branch are shown  
200 in Figure 3E. A VS branch and its input neurons are shown in Movie S1. The summary of these  
201 connectivity analyses (Figure 3F) shows that  $\sim 80\%$  of the input synapses of these cells are  
202 supplied by T4/T5. The HS (Lop1), VS (Lop4), and VS (Lop2) branches respectively receive  
203 7.14%, 18.9%, and 10.7% of the input synapses coming from bilayer LPi cells (Figure 3F, File  
204 S2). Intriguingly, the Lop2 VS branch receives inputs mainly from T4b, T5b, and LPi1-2 cells,  
205 suggesting it indeed receives back-to-front local motion signals. Overall, the connectivity pattern  
206 between the T4/T5, LPis, and the giant LPTCs is very similar in these different layers (Figure  
207 3E). This relatively simple connectivity structure strongly supports the expectations of previous  
208 functional studies of HS and VS cells—they appear to mainly integrate directionally selective  
209 inputs that are reinforced with motion opponent inputs from LPi neurons<sup>35</sup>.

210

### 211 **Connectivity of the bilayer Lobula Plate intrinsic (LPi) cells**

212 We identified four bilayer LPi neuron types as major T4/T5 targets (Figure 2A). A previous  
213 study described LPi3-4 and LPi4-3, and based on the functional importance of these neurons for  
214 motion opponency, speculated about the existence of all four types<sup>35</sup>. In this study, we have  
215 reconstructed and identified LPi1-2 and LPi2-1 that bridge Lop1 and Lop2, confirming these  
216 prior predictions, although we are unable to describe the complete morphology of these neurons.  
217 We found a strong candidate for LPi1-2 using LM (Figure S1A). This apparent match suggests

218 that LPi1-2, and perhaps also LPi2-1, may be considerably larger than LPi3-4 and LPi4-3.  
219 Confirming this proposal will require extensive reconstruction in a larger EM volume. All four  
220 LPi neuron types innervate two neighboring layers, with a stereotypic distribution of synapses  
221 (Figure 4, left). Each cell type has postsynaptic sites in one layer and presynaptic T-bars in the  
222 adjacent layer. At least 2/3 of the inputs are from layer-specific T4/T5 cells, while the outputs are  
223 shared by many neuron types (Figure 4, right; File S3). The LPi3-4 and LPi4-3 cells are  
224 glutamatergic<sup>35,41</sup>, and these cells provide inhibitory, directionally selective inputs to the target  
225 neurons<sup>35,37</sup>. Based on their similar morphology and connectivity, LPi1-2 and LPi2-1 are also  
226 likely inhibitory. This small circuit supports the proposed mechanism of Mauss et al.<sup>35</sup>: bilayer  
227 LPi cells integrate T4/T5 inputs in one layer and inhibit the postsynaptic neurons integrating the  
228 oppositely tuned T4/T5 signals in the adjacent layer, implementing motion opponency. The ~1/3  
229 of LPi inputs provided by cells other than T4/T5 suggest that the lobula plate circuitry is more  
230 complicated, and perhaps more flexible, than the circuit models consider, but future connectomic  
231 and functional studies will be required to understand how these additional neurons contribute to  
232 motion processing.

233

### 234 **Lobula plate Visual Projection Neurons (VPNs) that integrate T4 and T5 inputs**

235 In addition to the HS and VS cells (Figure 3), we identified several other VPns as T4/T5 targets  
236 (Figures 2 and 5). In this study, we focused on identifying and quantifying T4/T5 target neuron  
237 connectivity, rather than describing complete synaptic profiles of the VPns.

238

239 T4 and T5 connect with columnar VPns, smaller cells that as a population cover large parts of  
240 the lobula plate. These cells belong to three main groups (LPLC, LPC, and LLPC) that are  
241 distinguished by cell body location, innervation pattern in the optic lobe, and axonal path to the  
242 central brain (further explained in Figure 5 legend). Based on their arbor sizes in the lobula plate  
243 and T4/T5 inputs, these cells are expected to respond to visual motion signals within small  
244 patches of the fly's field of view. We distinguished two LPC types and three LLPC types based  
245 on lobula plate layer patterns (Figures 5A-E), in agreement with LM analyses<sup>44</sup>. LPC1 (Figure  
246 5A), receives inputs from T4b and T5b. This anatomy suggests that these cells integrate back-to-  
247 front motion signals, which has been confirmed by calcium imaging<sup>44</sup>. LPC2 (Figure 5B) is a  
248 small-field VPN with T4c/T5c inputs (Figure 2A) and is therefore predicted to encode upwards



249 motion. LLPC1 (Figure 5C), a VPN responsive to front-to-back visual motion<sup>44</sup>, has dendritic  
250 arbors in Lop1 and Lop3, with much stronger T4/T5 input in Lop1 (from T4a/T5a; Figure 2A).  
251 The synaptic terminal in the lobula appears to be mainly presynaptic (Figure 5C). LLPC2 and  
252 LLPC3 are similar cells with T4/T5 input in Lop3 and Lop4, respectively (Figures 5D-E).  
253 LPLC1 and LPLC2 cells<sup>38,40</sup> are notable for receiving T4/T5 inputs in multiple lobula plate  
254 layers: T4/T5 a, b, c, and d for LPLC2, in agreement with the described mechanism of looming  
255 sensitivity in this cell type<sup>3</sup> and T4/T5 b and d for LPLC1 (Figures 2A, 5F-G). By contrast,  
256 LPLC4<sup>38,40</sup> is not a strong T4/T5 target in our dataset.

257

258 T4 and T5 neurons connect with LPTCs other than HS and VS cells, some of which we matched  
259 to known neurons, but in other cases, we name them based on their layer innervation patterns  
260 (Figures 5H-O). As many LPTCs are morphologically unique, we expect that many of these cells  
261 could be matched, one-for-one, to LM images or other EM reconstructions<sup>34,53</sup>. The dorsal  
262 centrifugal horizontal (DCH) cell (Figure 5P) is unique among this group as it is predominantly  
263 presynaptic to T4 and T5 (Figure 2A): 15.3% of T4a inputs and 12.7% of T5a inputs (excluding  
264 synapses between T4/T5 terminals) are from DCH, and it is by far the largest input to T4/T5  
265 from a single LPTC. The terminals of DCH cover the dorsal half of Lop1, while the homologous  
266 ventral centrifugal horizontal (VCH) cell covers the ventral half<sup>34,54,55</sup>. The CH neurons innervate  
267 the ipsilateral inferior posterior slope (IPS) in the central brain, are GABAergic<sup>55-57</sup>, and likely  
268 inhibitory. Although we did not find VCH (due to the imaged area restriction), our data suggest  
269 that these two cells are the only major LPTCs that feed signals from the central brain to T4a/T5a  
270 (File S1).

271

272 H1 is a heterolateral LPTC directly connecting both lobula plates (Figure 5Q)<sup>28</sup>, and is sensitive  
273 to ipsilateral back-to-front visual motion, similar to H2<sup>58,59</sup>. We found two profiles that likely  
274 correspond to proximal and distal terminals of both H1 cells. The proximal terminal is  
275 predominantly postsynaptic and confined within Lop2, while the putative distal terminal branch  
276 is presynapse-rich, with boutons mainly in Lop1 and Lop2. T4b and T5b provide synaptic inputs  
277 to the proximal terminal, but H1 does not appear in Figure 2A since the averaged numbers of  
278 synapses per terminal (~4.8 from both T4b and T5b) were below our threshold for inclusion.  
279 Nonetheless, H1 is expected to integrate many inputs from T4b/T5b throughout Lop2, which is

280 consistent with the described motion preference<sup>28,54,58,59</sup>. The distal terminal of H1 has limited  
281 synaptic contacts with T4 or T5 cells (only accounting for ~0.1% of H1's predicted output  
282 synapses).

283  
284 The H2 cell, another identifiable LPTC that is well-known from work in larger flies, has dense  
285 neuronal processes confined to Lop2 (Figure 5R) and projects to the IPS in the contralateral  
286 hemisphere of the brain<sup>30,55</sup>. Unlike HS or VS cells, H2 branches in Lop2 feature mixed pre- and  
287 postsynaptic terminals (Figure 5R, inset), as suggested by genetically-driven synaptic markers<sup>55</sup>.  
288 H2 reportedly connects with the CH cells in the central brain<sup>58</sup>, and a central brain EM  
289 connectome dataset ("hemibrain") revealed that H2 provides the strongest input to DCH and  
290 VCH<sup>43</sup>. H2 is thus strongly coupled with the CH cells from the opposite brain hemisphere,  
291 contributing to processing motion information from both eyes.

292

### 293 **Optic lobe intrinsic neurons that integrate T4 and T5 inputs**

294

295 T4 and T5 target optic lobe intrinsic cells in addition to the bilayer LPi neurons, including  
296 several types of LPi, TmY, Y, and Tlp neurons (Figure 6). We identified both known and new  
297 optic lobe intrinsic cell types as we described T4/T5 targets. For most of the new cell types in  
298 this group, we further confirmed the morphology with LM matches (Figure S2).

299

300 One noteworthy target is Am1 (Figure 6A), a single, large, amacrine-like neuron innervating the  
301 medulla, lobula, and lobula plate with tree-like arborization<sup>27,45</sup>. Am1 receives inputs from  
302 T4b/T5b in Lop2 (Figure 2A) and has significant synaptic contacts with some LPTCs. The  
303 predicted synapses contain strong inputs from DCH and contralateral H1, and outputs to DCH  
304 and HS cells. Based on these connections, we expect that Am1 is inhibitory (since it is unlikely  
305 to excite HS cells in response to ipsilateral T4b/T5b input) and participates in a bilateral circuit  
306 comprised of several tangential cells that integrate horizontal motion signals from both eyes<sup>58-61</sup>  
307 (Figure 7C).

308

309 We find several putative LPi and LPi-like neuron types (Figures 6B-F) that all differ from the  
310 bilayer LPi types and provide further examples of the diverse neuronal composition of each

311 layer. A large cell we tentatively named LPT/LPi2a receives the strongest inputs from T4b and  
312 T5b among all the neurons in our data (Figures 2A and 6B). LPT/LPi2a has a similar but distinct  
313 morphology from the bilayer LPi2-1 cell in the lobula plate, with main branches containing pre-  
314 and postsynapses in Lop2 with additional sparser processes in Lop1. While T4/T5 supply >80%  
315 of LPi2-1's input, this number is <50% for LPT/LPi2a, suggesting it participates in circuits with  
316 more elaborate connectivity than the main bilayer LPis (Figure 7A). Our best candidate for an  
317 LM match is a VPN with a projection to the central brain (Figure S1B). LPi2b is another large  
318 Lop2 cell that appears to span the entire lobula plate, but with a more restricted layer pattern and  
319 fewer inputs from T4/T5 (Figures 6C and S1C). LPi34-12 (Figure 6C; named for its layer  
320 pattern) is similar to the bilayer LPi cells but receives T4/T5 input in both Lop3 and Lop4 and  
321 has output synapses in Lop1 and Lop2 (Figure 2A), and thus appears to represent an undescribed  
322 interaction between motion detected along different directions.

323

324 TmY cells have cell bodies in the medulla cell body rind and terminals in both the lobula and  
325 lobula plate (Figures 6G-L). TmY4, TmY5a, TmY14, and TmY15 have been previously  
326 described<sup>14,20-22</sup>, while TmY16 and TmY20 are reported here for the first time and confirmed  
327 with LM matches (Figures S2A-B). TmY20 has the highest number of inputs from T4a/T5a of  
328 all the targets we found (52.6 synapses/T4a and 66.6 synapses/ T5a; Figure 2A, File S1). Unlike  
329 most TmY cells, we don't find synapses on the TmY20 neurite in the medulla; the cell synapses  
330 only in the lobula and lobula plate (reminiscent of LPi3-4, which also lacks synapses in the  
331 medulla<sup>35</sup>). TmY20 has mostly presynaptic terminals in lobula layers Lo5 and Lo6 (Figure 6L),  
332 suggesting this neuron relays front-to-back motion information to lobula neurons. The other  
333 TmY cells have extensive arborizations outside the lobula plate and a full inventory of their  
334 connectivity may be required for detailed predictions about their role in motion processing. Y  
335 cells (Figures 6M-O) are columnar neurons with cell bodies in the rind posterior to the lobula  
336 plate, that innervate the medulla, lobula, and lobula plate<sup>14</sup>. Tlp cells (Figures 6J-S, S2E-H) are  
337 similar to Y-cells but lack a medulla branch. We identify one known (Y3) and two previously  
338 undescribed Y neurons (Y11, Y12) as T4/T5 targets, and confirm their morphology using LM  
339 (Figures S2C-D). Tlp, Y and TmY cells all provide paths for relaying different subsets of  
340 retinotopic T4/T5 outputs to the lobula (Figure 7D).

341

342 The two Y-cell types identified here, Y11 and Y12, are notable for integrating T4/T5 input from  
343 different layers: Y11 from Lop1 and Lop3 and Y12 from Lop1 and Lop4. The two cells are  
344 otherwise morphologically very similar, with boutons in the same medulla and lobula layers.  
345 Both cell types have pre- and postsynaptic contacts with T4 and T5 (File S1), integrating their  
346 signals in their respective layers. Since Y11 synthesizes front-to-back (Lop1) and upward (Lop3)  
347 motion signals and Y12 combines front-to-back and downward (Lop4) motion signals, the two  
348 cells are likely to each encode a preferred motion direction along the oblique directions in-  
349 between the preferred cardinal directions of their input T4s and T5s (Figure 7B).

350

## 351 **Discussion**

352

353 The giant tangential cells of the fly lobula plate have received considerable interest for  
354 decades<sup>30,62,63</sup>, but the descriptions of the circuits at this ‘final’ optic lobe stage of the motion  
355 pathway have been rather incomplete. In this study, we used 3D-EM reconstructions to inventory  
356 the synaptic partners of T4 and T5 neurons with completeness unmatched by other approaches.  
357 Our work reveals a much more elaborate architecture for processing visual motion, with several  
358 major new findings: 1) lobula plate target neurons integrate T4 and T5 inputs with approximately  
359 equal weights, 2) each layer houses a unique ensemble of downstream neurons, while sharing a  
360 core circuit motif composed of T4/T5, a bilayer LPi cell, and output VPNS, 3) new circuit  
361 elements that combine motion signals for different directions, including the Y11 and Y12 cells,  
362 and, 4) many neurons conveying motion signals from the lobula plate to the lobula, implicating  
363 lobula circuitry with a more significant role in motion processing.

364

365 We found that all lobula plate neurons that are strongly connected to T4 and T5 axon terminals  
366 integrate these inputs, in the same layers, with nearly equal weight (Figure 2B). This is a  
367 conceptually significant finding, as it implies, at least for the motion pathway, that the ON and  
368 OFF separation is an internal feature of the optic lobe, and at the output stages of the pathway,  
369 the ON and OFF motion signals are combined onto all prominent lobula plate targets.

370

371 Most of the identified LPTCs receive T4/T5 inputs in single layers, while three columnar VPNS  
372 (LLPC1, LPLC1, and LPLC2) and some optic lobe intrinsic neurons (e.g., LPi34-12) receive

373 T4/T5 inputs in multiple layers (Figure 2A, 5, 6). These connectivity patterns suggest that most  
374 LPTCs carry large-field motion information representing one of the four cardinal directions,  
375 while small-field neurons may integrate signals from multiple layers and as a population could  
376 transmit more complex motion information to their downstream neurons. The best explored  
377 example of this is LPLC2, whose looming sensitivity was attributed to T4/T5 and bilayer LPi  
378 inputs in all four layers<sup>2,3</sup>, a hypothesis that this study has substantively confirmed.

379

### 380 **Bilayer LPi cells**

381 Most neurons we describe, such as the LPTCs or the columnar cells, appeared variable across the  
382 layers, only T4, T5, and the bilayer LPi cells exist in nearly identical, layer-specific subtypes.  
383 The four bilayer LPi cells have a common distribution of synapses, with nearly equal T4/T5  
384 inputs in one layer, and substantial output synapses in a neighboring layer, where they  
385 presumably inhibit most or all of the neurons that also receive excitatory T4/T5 inputs in that  
386 layer (Figures 2A, 4, and 7A), implementing motion opponency<sup>35</sup>. While the bilayer LPi cell  
387 types likely serve similar functions in motion processing, there are also clear anatomical  
388 differences. The cell bodies of LPi1-2, LPi2-1, and LPi4-3 are in the lobula plate cortex, while  
389 LPi3-4's are in the medulla cortex<sup>14,22,35</sup>, and therefore likely derive from different precursor  
390 cells. EM and LM data suggest that there are substantial size differences among the bilayer LPis,  
391 with LPi3-4 likely the smallest arborization, and individual LPi1-2 cells potentially arborizing  
392 across much of the lobula plate (Figure S1A). Since the spatial coverage of individual LPi  
393 neurons differs between the four types, the spatial integration of opponent signals may differ  
394 between layers, for reasons that are unclear and merit further investigation. These differences  
395 raise questions about the evolution of the bilayer LPi cells. Are these LPis derived from a shared  
396 ancestral cell type, for example via duplication, that later substantially diverged in some of their  
397 anatomical properties? Or did the antiparallel inhibition mediated by the bilayer LPis evolve  
398 independently in different layers?

399

### 400 **Y cells encoding oblique motion directions**

401 We discovered that Y11 and Y12 integrate motion information in two layers and thus likely  
402 synthesize a preferred tuning for a new, oblique direction of motion (Figures 2A and 7B). These  
403 neurons effectively fill two gaps between the four cardinal directions represented by T4/T5

404 subtypes. Both neurons combine a vertical motion signal with front-to-back motion, but we did  
405 not find complementary neurons for the oblique motion directions integrating Lop2/back-to-front  
406 motion. This asymmetry may reflect a bias for motion components experienced during forward  
407 locomotion. The Y cells have some similarities but also large differences with LPLC2, as they  
408 receive T4/T5 inputs from spatially overlapping areas in different layers, and their main targets  
409 are in the lobula and medulla (Figures 6N,O, and 7D). Taken together, this suggests that Y11 and  
410 Y12 likely synthesize ‘new’ preferred directions of motion sensitivity which is then further  
411 processed or integrated with other visual modalities. Identifying the targets of Y11 and Y12 will  
412 be an important goal of future connectomes.

413

#### 414 **Expanding the horizontal motion detection circuit with new cell types**

415 Our detailed analysis of the neurons connected to T4/T5 in Lop1 and Lop2 suggests several new  
416 connections should be added to existing models of binocular integration of rotational optic flow  
417 derived from work in blowflies<sup>61</sup>. The Am1 cell, which receives inputs from ipsilateral T4b/T5b  
418 and contralateral H1, likely combines optic flow across both eyes. H1 expresses a marker for  
419 glutamatergic neurons<sup>55</sup>. In *Drosophila*, glutamate could function as either an excitatory or  
420 inhibitory transmitter, while in blowfly, H1 seems to provide excitatory signals<sup>58</sup>. T4b and T5b  
421 detect back-to-front movement, and via (putative) inhibitory LPi2-1 cells, suppress the activity of  
422 neurons in Lop1, including HS cells (Figure 7C). Am1 may represent two more pathways for  
423 suppressing the activity of HS cells in response to back-to-front motion inputs, directly, and  
424 through DCH, which is also electrically coupled with HS in *Calliphora*<sup>61</sup>. It would appear that  
425 opponency is accomplished at different scales—the scale of bilayer LPi neurons and the CH  
426 neurons, and over the entire field of view by combining contralateral optic flow transmitted by  
427 H1 and H2 (Figure 7C).

428

#### 429 **Multiple neuron types convey T4/T5 signals to specific lobula layers**

430 Our analysis shows that T4/T5 have strong synaptic contacts with a variety of neuron types that  
431 appear to relay these signals within the optic lobe. For example, TmY20 cells (Figure 6L),  
432 receive the largest share of T4a/T5a output synapses (Figure 2A). While the standard circuit  
433 models of the motion pathways, comprised of T4/T5, LPTCs, and bilayer interneurons (Figure  
434 7A), have remained compact, evidence for additional, strong pathways suggests a broader role

435 for motion signals. A substantial fraction of T4/T5 downstream cells, including Tlp, LLPC, and  
436 TmY neurons (Figures 2, 5, and 6) project to the lobula, where they mainly target layer Lo4  
437 (Figure 7D). The circuits of the lobula, outside of the T5 inputs in Lo1, have been scarcely  
438 examined. What is now clear is that motion signals passed from the lobula plate should  
439 significantly contribute to visual pathways in the lobula, and potentially many VPNs projecting  
440 to the central brain could inherit motion signals from the lobula plate without any input sites  
441 there. The complete description of these pathways and their extended circuits will require an EM  
442 data set that covers all neuropils of the optic lobe as well as the central brain.

443

#### 444 **Towards complete reconstruction of sensory-to-motor pathways**

445 The connectivity profile of T4/T5 in the lobula plate we present here fills a large missing part of  
446 the motion pathways, the link between the detection of directionally selective motion and visual  
447 projection neurons of the lobula plate. With this part finally reconstructed, the motion pathway  
448 from the photoreceptor cells to the central brain can now be traced neuron-by-neuron by  
449 combining the accomplishments of multiple 3D-EM reconstructions<sup>18-20,22,23,64</sup>. Many of the  
450 VPNs we reconstructed here are also identified in the hemibrain dataset<sup>43</sup> that contains much of  
451 the central brain, enabling the comprehensive identification of downstream circuits to extend the  
452 described pathways even further. Many of the new discoveries reported here suggest a more  
453 integrative picture of optic lobe processing, where the lobula plate is no longer seen as the sole  
454 substrate for motion processing, but rather is understood to organize ON and OFF directionally  
455 selective signals for a variety of as-yet unexplored roles in visually guided behaviors.

456

#### 457 **Acknowledgements**

458 The authors thank members of the FlyEM Project Team at Janelia Research Campus for sample  
459 preparation, image acquisition, image processing, and proofreading of the neurons and synapses  
460 and the FlyLight Project Team for light microscopy images. We especially thank Stuart Berg,  
461 Lowell Umayam, and William Katz of the FlyEM Team for data management and preparing  
462 neuPrint/neuroglancer data, and Gerry Rubin and the members of the FlyEM steering committee  
463 for supporting this project. We also thank members of the Reiser lab for fruitful discussions and  
464 advice on the analysis. This project was supported by HHMI.

## 465 **Methods**

### 466 **The EM dataset**

467 All of the results presented in this manuscript were based on the same optic lobe FIB-SEM  
468 data volume that was used in two previous studies<sup>22,45</sup>. The sample was obtained from the right  
469 optic lobe of a 6-day post-eclosion female fruit fly, *Drosophila melanogaster*, a cross between  
470 homozygous *w<sup>1118</sup>* and CS wild type. The tissue was imaged with FIB-SEM with an isotropic  
471 voxel resolution ( $x = y = z = 8$  nm). The size of the image stack is  $19,162 \times 10,657 \times 22,543$   
472 pixels, equivalent to  $153 \mu\text{m} \times 85 \mu\text{m} \times 180 \mu\text{m}$  of the brain. The grayscale data of the image  
473 volume as well as the reconstructed neurons is available at <http://emdata.janelia.org/optic-lobe/>.  
474 Connectivity data will be made available through neuPrint, an online tool for accessing and  
475 analyzing connectome data<sup>65</sup>. For more information, see the **EM reconstruction of synaptic**  
476 **partners of T4 and T5 cells in the lobula plate** section and our previous publication<sup>22</sup>.

477

### 478 **Reconstruction of the neurons and the neuron nomenclature**

479 Neuronal profiles were automatically segmented, and synaptic motifs (presynaptic T-bars  
480 and postsynaptic densities) were predicted throughout the volume as described previously<sup>22</sup>.  
481 Predicted synapses reliably reveal connectivity of most neurons and polarity of most synaptic  
482 connections<sup>22</sup>, while they include some false-positive and false-negative synapses. For the main  
483 connectivity results analyzed and presented here, we manually proofread all predicted pre- and  
484 postsynapses of the 40 core T4 and T5 neurons as well as the dendrite fragments of the HS and  
485 VS cells (Figure 3) and the bilayer LPi cells (Figure 4) for higher quality results. Neurons and  
486 synapses were proofread and visualized using the NeuTu<sup>66</sup> software package.

487 After identifying representative T4 and T5 cells, five cells per each subtype, their synaptic  
488 partners in the lobula plate were exhaustively traced, though not necessarily to completion. Most  
489 of the cells documented in previous studies, including prominent LPTCs, were identified by their  
490 morphology. When two or more neurons have similar morphology, information of the spatial  
491 distributions of pre- and postsynaptic terminals, synapse counts, as well as the neuron types  
492 sharing synaptic connections were used to determine the cell types. New neuron types identified  
493 in this work (part of Figures 5 and 6) were named following the nomenclature convention of the  
494 optic lobe neurons primarily introduced by Fischbach and Dittrich<sup>14</sup>. The lobula plate tangential  
495 cells (LPTCs) have traditionally been given unique names, such as the HS, VS, and CH cells.  
496 Newly found LPTCs were distinguished by the extent of branching arbors in the lobula plate.  
497 Using a similar format used by Fischbach and Dittrich<sup>14</sup> and Otsuna and Ito<sup>67</sup> for other neuron  
498 types, we tentatively named these cells by combining LPT (lobula plate tangential) + innervating  
499 layers + alphabetical identifier, e.g., LPT3b and LPT34a. This nomenclature aligns with neuron  
500 names such as the lobula tangential (LT), medulla tangential (MT), and lobula columnar (LC)  
501 cells, while using “C” for “cell” was avoided for naming individual neurons as it is commonly  
502 used to abbreviate “columnar”. Likewise, the names for the columnar lobula plate cells, LPC,  
503 LLPC, and LPLC, match the names used in other studies carried out at the Janelia Research  
504 Campus<sup>38,43,44</sup>. Neurons were given tentative names as far as the overall morphology was



505 reconstructed or, at least, a characteristic branch in the lobula plate was sufficiently reconstructed  
506 (in the case of LPi and LPTCs). Numbers used in the names of the Tlp and Y cells were selected  
507 to avoid overlap with numbers in Fischbach and Dittrich<sup>14</sup> (since EM/Golgi matches can be  
508 inclusive). Gaps in the numbering of TmY neuron types reflect cell types identified in ongoing  
509 work that are not T4 or T5 synaptic partners by the criteria used in this study and therefore are  
510 not included here. In contrast to the bilayer LPi names, the names of the TmY, Tlp, Y cells, etc.  
511 do not refer to the lobula plate layer pattern of these neurons.

512

### 513 **Light microscopy (LM) and LM/EM comparison**

514 Individual cells were labeled using MultiColorFlpOut (MCFO)<sup>16</sup>. Details of the fly crosses for  
515 each supporting figure panel are listed in Table S1. All images show cells from female flies.  
516 Images were acquired on Zeiss LSM 710 or 780 confocal microscopes with  $63 \times 1.4$  NA  
517 objectives at  $0.19 \mu\text{m} \times 0.19 \mu\text{m} \times 0.38 \mu\text{m}$  or  $0.38 \mu\text{m} \times 0.38 \mu\text{m} \times 0.38 \mu\text{m}$  voxel size. Samples  
518 were prepared and imaged by the Janelia FlyLight Project Team. Detailed protocols are  
519 available online (<https://www.janelia.org/project-team/flylight/protocols>). We used GAL4 lines  
520 from the Janelia and Vienna Tiles collections<sup>11,17</sup>. Figures show views of substacks rendered  
521 using VVD viewer ([https://github.com/takashi310/VVD\\_Viewer](https://github.com/takashi310/VVD_Viewer)). In some cases, additional  
522 labeled cells or background signal were removed by manual editing in VVD viewer. Original  
523 confocal stacks will be made available online.

524 LM and EM matches are based on visually comparing anatomical features, in particular cell  
525 body location and arborizations in specific optic lobe subregions and layers. With the exception  
526 of LPi2c and LPi3a (which we did not attempt to match due to their comparatively few distinct  
527 features and small size) and LPi2-1 (for which we did not identify LM images), we confirmed  
528 the cell shapes of all newly identified optic lobe intrinsic cell types by identifying probable light  
529 microscopy matches.

## 530 References

- 531 1. Borst, A., Haag, J., and Reiff, D.F. (2010). Fly Motion Vision. *Annual Review of Neuroscience* 33, 49-70.  
532 10.1146/annurev-neuro-060909-153155.
- 533 2. Ache, J.M., Polsky, J., Alghailani, S., Parekh, R., Breads, P., Peek, M.Y., Bock, D.D., von Reyn, C.R., and Card,  
534 G.M. (2019). Neural Basis for Looming Size and Velocity Encoding in the *Drosophila* Giant Fiber Escape  
535 Pathway. *Current Biology* 29, 1073-1081.e1074. <https://doi.org/10.1016/j.cub.2019.01.079>.
- 536 3. Klapoetke, N.C., Nern, A., Peek, M.Y., Rogers, E.M., Breads, P., Rubin, G.M., Reiser, M.B., and Card, G.M.  
537 (2017). Ultra-selective looming detection from radial motion opponency. *Nature* 551, 237-241.  
538 10.1038/nature24626.
- 539 4. Morimoto, M.M., Nern, A., Zhao, A., Rogers, E.M., Wong, A.M., Isaacson, M.D., Bock, D.D., Rubin, G.M., and  
540 Reiser, M.B. (2020). Spatial readout of visual looming in the central brain of *Drosophila*. *Elife* 9.  
541 10.7554/eLife.57685.
- 542 5. Song, B.M., and Lee, C.H. (2018). Toward a Mechanistic Understanding of Color Vision in Insects. *Front*  
543 *Neural Circuits* 12, 16. 10.3389/fncir.2018.00016.
- 544 6. Schnaitmann, C., Haikala, V., Abraham, E., Oberhauser, V., Thestrup, T., Griesbeck, O., and Reiff, D.F. (2018).  
545 Color Processing in the Early Visual System of *Drosophila*. *Cell* 172, 318-330 e318. 10.1016/j.cell.2017.12.018.
- 546 7. Behnia, R., Clark, D.A., Carter, A.G., Clandinin, T.R., and Desplan, C. (2014). Processing properties of ON and  
547 OFF pathways for *Drosophila* motion detection. *Nature* 512, 427-430. 10.1038/nature13427.
- 548 8. Maisak, M.S., Haag, J., Ammer, G., Serbe, E., Meier, M., Leonhardt, A., Schilling, T., Bahl, A., Rubin, G.M.,  
549 Nern, A., et al. (2013). A directional tuning map of *Drosophila* elementary motion detectors. *Nature* 500, 212-  
550 216. 10.1038/nature12320.
- 551 9. Brand, A.H., and Perrimon, N. (1993). Targeted gene expression as a means of altering cell fates and generating  
552 dominant phenotypes. *development* 118, 401-415.
- 553 10. Duffy, J.B. (2002). GAL4 system in *Drosophila*: a fly geneticist's Swiss army knife. *Genesis* 34, 1-15.  
554 10.1002/gene.10150.
- 555 11. Jenett, A., Rubin, G.M., Ngo, T.T., Shepherd, D., Murphy, C., Dionne, H., Pfeiffer, B.D., Cavallaro, A., Hall, D.,  
556 Jeter, J., et al. (2012). A GAL4-driver line resource for *Drosophila* neurobiology. *Cell Rep* 2, 991-1001.  
557 10.1016/j.celrep.2012.09.011.
- 558 12. Simpson, J.H. (2016). Rationally subdividing the fly nervous system with versatile expression reagents. *J*  
559 *Neurogenet* 30, 185-194. 10.1080/01677063.2016.1248761.
- 560 13. Borst, A. (2009). *Drosophila*'s view on insect vision. *Curr Biol* 19, R36-47. 10.1016/j.cub.2008.11.001.
- 561 14. Fischbach, K.-F., and Dittrich, A. (1989). The optic lobe of *Drosophila melanogaster*. I. A Golgi analysis of  
562 wild-type structure. *Cell and tissue research* 258, 441-475.
- 563 15. Strausfeld, N.J. (1976). *Atlas of an insect brain* (Springer-Verlag).
- 564 16. Nern, A., Pfeiffer, B.D., and Rubin, G.M. (2015). Optimized tools for multicolor stochastic labeling reveal  
565 diverse stereotyped cell arrangements in the fly visual system. *Proc Natl Acad Sci U S A* 112, E2967-2976.  
566 10.1073/pnas.1506763112.
- 567 17. Tirian, L., and Dickson, B. (2017). The VT GAL4, LexA, and split-GAL4 driver line collections for targeted  
568 expression in the *Drosophila* nervous system. *bioRxiv*. 10.1101/198648.
- 569 18. Rivera-Alba, M., Vitaladevuni, S.N., Mishchenko, Y., Lu, Z., Takemura, S.Y., Scheffer, L., Meinertzhagen, I.A.,  
570 Chklovskii, D.B., and de Polavieja, G.G. (2011). Wiring economy and volume exclusion determine neuronal  
571 placement in the *Drosophila* brain. *Curr Biol* 21, 2000-2005. 10.1016/j.cub.2011.10.022.
- 572 19. Takemura, S.Y., Lu, Z., and Meinertzhagen, I.A. (2008). Synaptic circuits of the *Drosophila* optic lobe: the input  
573 terminals to the medulla. *J Comp Neurol* 509, 493-513. 10.1002/cne.21757.
- 574 20. Takemura, S.Y., Bharioke, A., Lu, Z., Nern, A., Vitaladevuni, S., Rivlin, P.K., Katz, W.T., Olbris, D.J., Plaza,  
575 S.M., Winston, P., et al. (2013). A visual motion detection circuit suggested by *Drosophila* connectomics. *Nature*  
576 500, 175-181. 10.1038/nature12450.
- 577 21. Takemura, S.Y., Nern, A., Chklovskii, D.B., Scheffer, L.K., Rubin, G.M., and Meinertzhagen, I.A. (2017). The  
578 comprehensive connectome of a neural substrate for 'ON' motion detection in *Drosophila*. *eLife* 6, e24394.  
579 10.7554/eLife.24394.
- 580 22. Shinomiya, K., Huang, G., Lu, Z., Parag, T., Xu, C.S., Aniceto, R., Ansari, N., Cheatham, N., Lauchie, S.,  
581 Neace, E., et al. (2019). Comparisons between the ON- and OFF-edge motion pathways in the *Drosophila* brain.  
582 *eLife* 8, e40025. 10.7554/eLife.40025.
- 583 23. Shinomiya, K., Karuppururai, T., Lin, T.Y., Lu, Z., Lee, C.H., and Meinertzhagen, I.A. (2014). Candidate neural  
584 substrates for off-edge motion detection in *Drosophila*. *Curr Biol* 24, 1062-1070. 10.1016/j.cub.2014.03.051.

- 585 24. Strother, J.A., Wu, S.T., Wong, A.M., Nern, A., Rogers, E.M., Le, J.Q., Rubin, G.M., and Reiser, M.B. (2017).  
586 The emergence of directional selectivity in the visual motion pathway of *Drosophila*. *Neuron* 94, 168-182 e110.  
587 10.1016/j.neuron.2017.03.010.
- 588 25. Serbe, E., Meier, M., Leonhardt, A., and Borst, A. (2016). Comprehensive characterization of the major  
589 presynaptic elements to the *Drosophila* OFF motion detector. *Neuron* 89, 829-841.  
590 10.1016/j.neuron.2016.01.006.
- 591 26. Strausfeld, N.J. (2021). The lobula plate is exclusive to insects. *Arthropod Struct Dev* 61, 101031.  
592 10.1016/j.asd.2021.101031.
- 593 27. Hausen, K., and Egelhaaf, M. (1989). Neural Mechanisms of Visual Course Control in Insects. held in Berlin,  
594 Heidelberg, 1989//. D.G. Stavenga, and R.C. Hardie, eds. (Springer Berlin Heidelberg), pp. 391-424.
- 595 28. Hausen, K. (1984). The Lobula-Complex of the Fly: Structure, Function and Significance in Visual Behaviour.  
596 In *Photoreception and Vision in Invertebrates*, M.A. Ali, ed. (Springer US), pp. 523-559. 10.1007/978-1-4613-  
597 2743-1\_15.
- 598 29. Eckert, H. (1980). Functional properties of the H1-neurone in the third optic Ganglion of the Blowfly, *Phaenicia*.  
599 *Journal of comparative physiology* 135, 29-39. 10.1007/BF00660179.
- 600 30. Hausen, K. (1976). Functional characterization and anatomical identification of motion sensitive neurons in the  
601 lobula plate of the blowfly *Calliphora erythrocephala*. *Zeitschrift für Naturforschung c* 31, 629-634.
- 602 31. Scott, E.K., Raabe, T., and Luo, L. (2002). Structure of the vertical and horizontal system neurons of the lobula  
603 plate in *Drosophila*. *J Comp Neurol* 454, 470-481. 10.1002/cne.10467.
- 604 32. Joesch, M., Plett, J., Borst, A., and Reiff, D.F. (2008). Response properties of motion-sensitive visual  
605 interneurons in the lobula plate of *Drosophila melanogaster*. *Curr Biol* 18, 368-374. 10.1016/j.cub.2008.02.022.
- 606 33. Schnell, B., Joesch, M., Forstner, F., Raghu, S.V., Otsuna, H., Ito, K., Borst, A., and Reiff, D.F. (2010).  
607 Processing of horizontal optic flow in three visual interneurons of the *Drosophila* brain. *J Neurophysiol* 103,  
608 1646-1657. 10.1152/jn.00950.2009.
- 609 34. Boergens, K.M., Kapfer, C., Helmstaedter, M., Denk, W., and Borst, A. (2018). Full reconstruction of large  
610 lobula plate tangential cells in *Drosophila* from a 3D EM dataset. *PLoS One* 13, e0207828.  
611 10.1371/journal.pone.0207828.
- 612 35. Mauss, A.S., Pankova, K., Arenz, A., Nern, A., Rubin, G.M., and Borst, A. (2015). Neural circuit to integrate  
613 opposing motions in the visual field. *Cell* 162, 351-362. 10.1016/j.cell.2015.06.035.
- 614 36. Raghu, S.V., and Borst, A. (2011). Candidate glutamatergic neurons in the visual system of *Drosophila*. *PLoS*  
615 *One* 6, e19472. 10.1371/journal.pone.0019472.
- 616 37. Mauss, A.S., Meier, M., Serbe, E., and Borst, A. (2014). Optogenetic and pharmacologic dissection of  
617 feedforward inhibition in *Drosophila* motion vision. *J Neurosci* 34, 2254-2263. 10.1523/JNEUROSCI.3938-  
618 13.2014.
- 619 38. Wu, M., Nern, A., Williamson, W.R., Morimoto, M.M., Reiser, M.B., Card, G.M., and Rubin, G.M. (2016).  
620 Visual projection neurons in the *Drosophila* lobula link feature detection to distinct behavioral programs. *eLife*  
621 5. 10.7554/eLife.21022.
- 622 39. Gilbert, C., and Strausfeld, N.J. (1991). The functional organization of male-specific visual neurons in flies. *J*  
623 *Comp Physiol A* 169, 395-411. 10.1007/BF00197653.
- 624 40. Panser, K., Tirian, L., Schulze, F., Villalba, S., Jefferis, G., Buhler, K., and Straw, A.D. (2016). Automatic  
625 Segmentation of *Drosophila* Neural Compartments Using GAL4 Expression Data Reveals Novel Visual  
626 Pathways. *Curr Biol* 26, 1943-1954. 10.1016/j.cub.2016.05.052.
- 627 41. Davis, F.P., Nern, A., Picard, S., Reiser, M.B., Rubin, G.M., Eddy, S.R., and Henry, G.L. (2020). A genetic,  
628 genomic, and computational resource for exploring neural circuit function. *Elife* 9. 10.7554/eLife.50901.
- 629 42. Strausfeld, N.J., and Okamura, J.Y. (2007). Visual system of calliphorid flies: organization of optic glomeruli  
630 and their lobula complex efferents. *J Comp Neurol* 500, 166-188. 10.1002/cne.21196.
- 631 43. Scheffer, L.K., Xu, C.S., Januszewski, M., Lu, Z., Takemura, S.Y., Hayworth, K.J., Huang, G.B., Shinomiya, K.,  
632 Maitlin-Shepard, J., Berg, S., et al. (2020). A connectome and analysis of the adult *Drosophila* central brain.  
633 *eLife* 9. 10.7554/eLife.57443.
- 634 44. Isaacson MD, Eliason JLM, Nern A, Rogers EM, Rubin GM, Branson K, and MB, R. (in preparation). Small-  
635 field visual projection neurons detect translational optic flow and contribute to the regulation of forward walking.
- 636 45. Shinomiya, K., Horne, J.A., McLin, S., Wiederman, M., Nern, A., Plaza, S.M., and Meinertzhagen, I.A. (2019).  
637 The Organization of the Second Optic Chiasm of the *Drosophila* Optic Lobe. *Front Neural Circuits* 13, 65.  
638 10.3389/fncir.2019.00065.
- 639 46. Haag, J., Vermeulen, A., and Borst, A. (1999). The intrinsic electrophysiological characteristics of fly lobula  
640 plate tangential cells: III. Visual response properties. *J Comput Neurosci* 7, 213-234. 10.1023/a:1008950515719.

- 641 47. Krapp, H.G., and Hengstenberg, R. (1996). Estimation of self-motion by optic flow processing in single visual  
642 interneurons. *Nature* 384, 463-466. 10.1038/384463a0.
- 643 48. Hengstenberg, R. (1982). Common visual response properties of giant vertical cells in the lobula plate of the  
644 blowfly *Calliphora*. *Journal of comparative physiology* 149, 179-193. 10.1007/BF00619212.
- 645 49. Pierantoni, R. (1976). A look into the cock-pit of the fly. The architecture of the lobular plate. *Cell Tissue Res*  
646 171, 101-122. 10.1007/BF00219703.
- 647 50. Hengstenberg, R., Hausen, K., and Hengstenberg, B. (2004). The number and structure of giant vertical cells  
648 (VS) in the lobula plate of the blowfly *Calliphora erythrocephala*. *Journal of comparative physiology* 149, 163-  
649 177.
- 650 51. Kim, A.J., Fenk, L.M., Lyu, C., and Maimon, G. (2017). Quantitative Predictions Orchestrate Visual Signaling  
651 in *Drosophila*. *Cell* 168, 280-294 e212. 10.1016/j.cell.2016.12.005.
- 652 52. Barnhart, E.L., Wang, I.E., Wei, H., Desplan, C., and Clandinin, T.R. (2018). Sequential Nonlinear Filtering of  
653 Local Motion Cues by Global Motion Circuits. *Neuron* 100, 229-243 e223. 10.1016/j.neuron.2018.08.022.
- 654 53. Zheng, Z., Lauritzen, J.S., Perlman, E., Robinson, C.G., Nichols, M., Milkie, D., Torrens, O., Price, J., Fisher,  
655 C.B., Sharifi, N., et al. (2018). A Complete Electron Microscopy Volume of the Brain of Adult *Drosophila*  
656 *melanogaster*. *Cell* 174, 730-743 e722. 10.1016/j.cell.2018.06.019.
- 657 54. Eckert, H., and Dvorak, D.R. (1983). The centrifugal horizontal cells in the lobula plate of the blowfly,  
658 *Phaenicia sericata*. *Journal of Insect Physiology* 29, 547-560.
- 659 55. Wei, H., Kyung, H.Y., Kim, P.J., and Desplan, C. (2020). The diversity of lobula plate tangential cells (LPTCs)  
660 in the *Drosophila* motion vision system. *J Comp Physiol A Neuroethol Sens Neural Behav Physiol* 206, 139-  
661 148. 10.1007/s00359-019-01380-y.
- 662 56. Gauck, V., Egelhaaf, M., and Borst, A. (1997). Synapse distribution on VCH, an inhibitory, motion-sensitive  
663 interneuron in the fly visual system. *J Comp Neurol* 381, 489-499.
- 664 57. Meyer, E.P., Matute, C., Streit, P., and Nassel, D.R. (1986). Insect optic lobe neurons identifiable with  
665 monoclonal antibodies to GABA. *Histochemistry* 84, 207-216. 10.1007/BF00495784.
- 666 58. Haag, J., and Borst, A. (2001). Recurrent network interactions underlying flow-field selectivity of visual  
667 interneurons. *J Neurosci* 21, 5685-5692.
- 668 59. Farrow, K., Haag, J., and Borst, A. (2003). Input organization of multifunctional motion-sensitive neurons in the  
669 blowfly. *J Neurosci* 23, 9805-9811.
- 670 60. Duistermars, B.J., Care, R.A., and Frye, M.A. (2012). Binocular interactions underlying the classic optomotor  
671 responses of flying flies. *Front Behav Neurosci* 6, 6. 10.3389/fnbeh.2012.00006.
- 672 61. Farrow, K., Haag, J., and Borst, A. (2006). Nonlinear, binocular interactions underlying flow field selectivity of  
673 a motion-sensitive neuron. *Nat Neurosci* 9, 1312-1320. 10.1038/nn1769.
- 674 62. Bishop, C.A., and Bishop, L.G. (1981). Vertical motion detectors and their synaptic relations in the third optic  
675 lobe of the fly. *J Neurobiol* 12, 281-296. 10.1002/neu.480120308.
- 676 63. Dvorak, D.R., Bishop, L.G., and Eckert, H.E. (1975). On the identification of movement detectors in the fly  
677 optic lobe. *Journal of comparative physiology* 100, 5-23.
- 678 64. Takemura, S.-y., Xu, C.S., Lu, Z., Rivlin, P.K., Parag, T., Olbris, D.J., Plaza, S., Zhao, T., Katz, W.T., Umayam,  
679 L., et al. (2015). Synaptic circuits and their variations within different columns in the visual system of  
680 *Drosophila*. *Proceedings of the National Academy of Sciences* 112, 13711-13716. 10.1073/pnas.1509820112.
- 681 65. Clements, J., Dolafi, T., Umayam, L., Neubarth, N.L., Berg, S., Scheffer, L.K., and Plaza, S.M. (2020). *neuPrint*:  
682 Analysis Tools for EM Connectomics. *bioRxiv*, 2020.2001.2016.909465. 10.1101/2020.01.16.909465.
- 683 66. Feng, L., Zhao, T., and Kim, J. (2015). *neuTube 1.0*: a new design for efficient neuron reconstruction software  
684 based on the SWC format. *eneuro* 2, ENEURO.0049-0014.2014.
- 685 67. Otsuna, H., and Ito, K. (2006). Systematic analysis of the visual projection neurons of *Drosophila melanogaster*.  
686 I. Lobula-specific pathways. *J Comp Neurol* 497, 928-958. 10.1002/cne.21015.

687

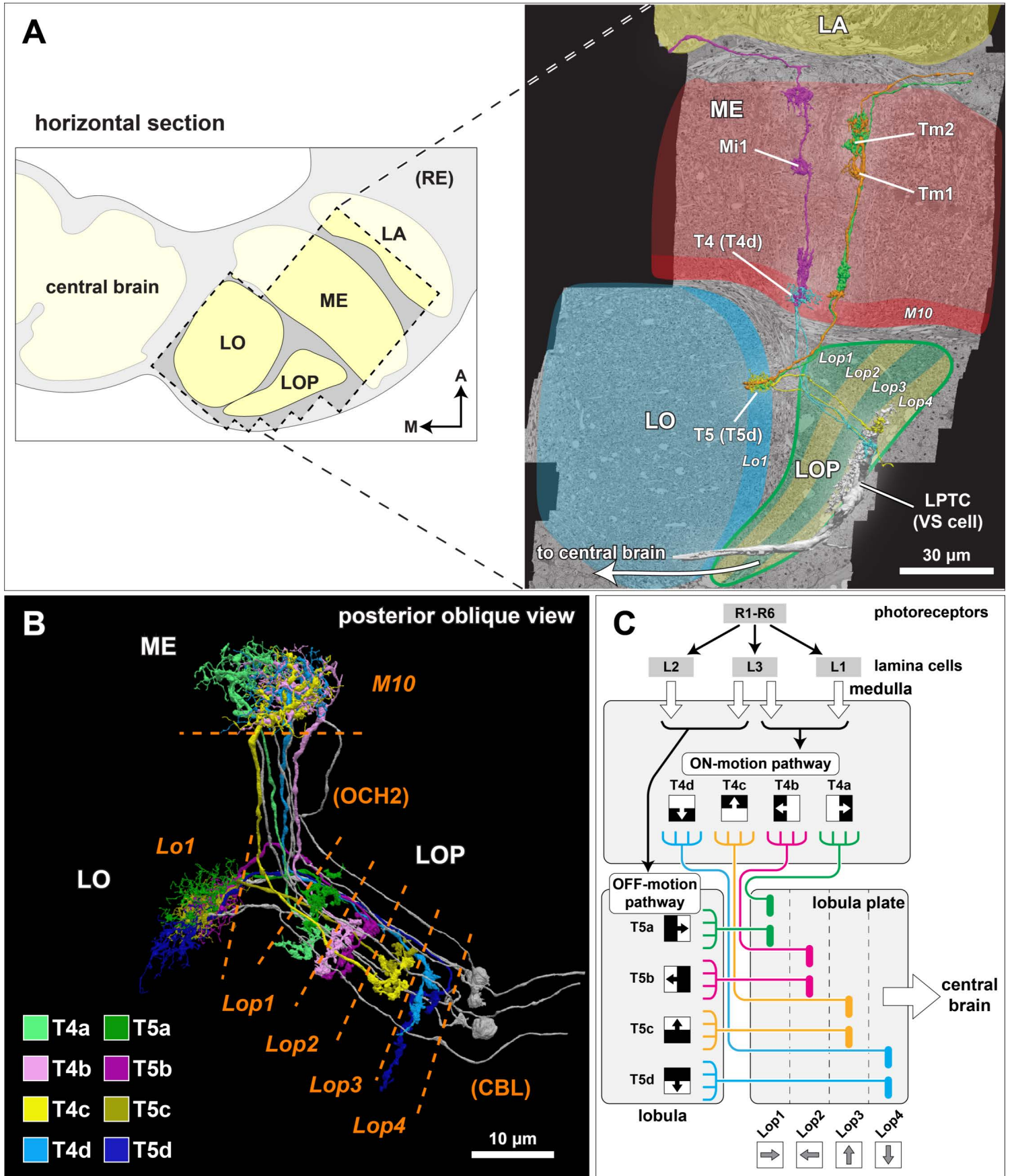


## **Figure 1. EM reconstruction of the synaptic partners of T4 and T5 cells in the lobula plate.**

(A) The optic lobe FIB-SEM dataset covers a subvolume of the medulla (ME), lobula (LO), and lobula plate (LOP), as well as the proximal part of the lamina (LA), selected to contain many connected neurons of the motion pathway. The data set was imaged with voxel size  $x = y = z = 8$  nm, and the size of the image stack is  $19,162 \times 10,657 \times 22,543$  pixels, equivalent to  $153 \mu\text{m} \times 85 \mu\text{m} \times 180 \mu\text{m}$  <sup>22</sup>. In the right panel, representative neurons in the ON- and OFF-motion pathways in the medulla and the lobula, as well as a lobula plate tangential cell (VS cell) are shown (panel adapted from Shinomiya et al. <sup>22</sup>). M: medial, A: anterior. (B) Subtypes of the T4 and T5 cells. The T4 cells receive inputs onto their dendrites in medulla layer 10 (M10), T5 neurons receive dendritic input in lobula layer 1 (Lo1). Both cell types project through the non-synaptic second optic chiasm (OCH2) and stratify into the four layers of the lobula plate (Lop1-Lop4). The cell bodies are located at the cell body layer (CBL) in the lobula plate cortex. The cell bodies and the cell body fibers are shown in gray, while some cell bodies are not shown. (C) A schematic diagram of the motion circuit. Local luminance is detected by the photoreceptors R1-R6 in the retina. The signals are relayed to the lamina cells (L1, L2, and L3), which send outputs to various columnar cells in the medulla (not detailed here). The 4<sup>th</sup> order T4 and T5 neurons integrate inputs from the ON and OFF motion pathway neurons, respectively, and project to the lobula plate. The four subtypes (a, b, c, and d) detect visual motion in the front-to-back, back-to-front, upward, and downward directions, respectively, and project axons to the corresponding LOP layer where these directionally selective signals are integrated by lobula plate neurons.

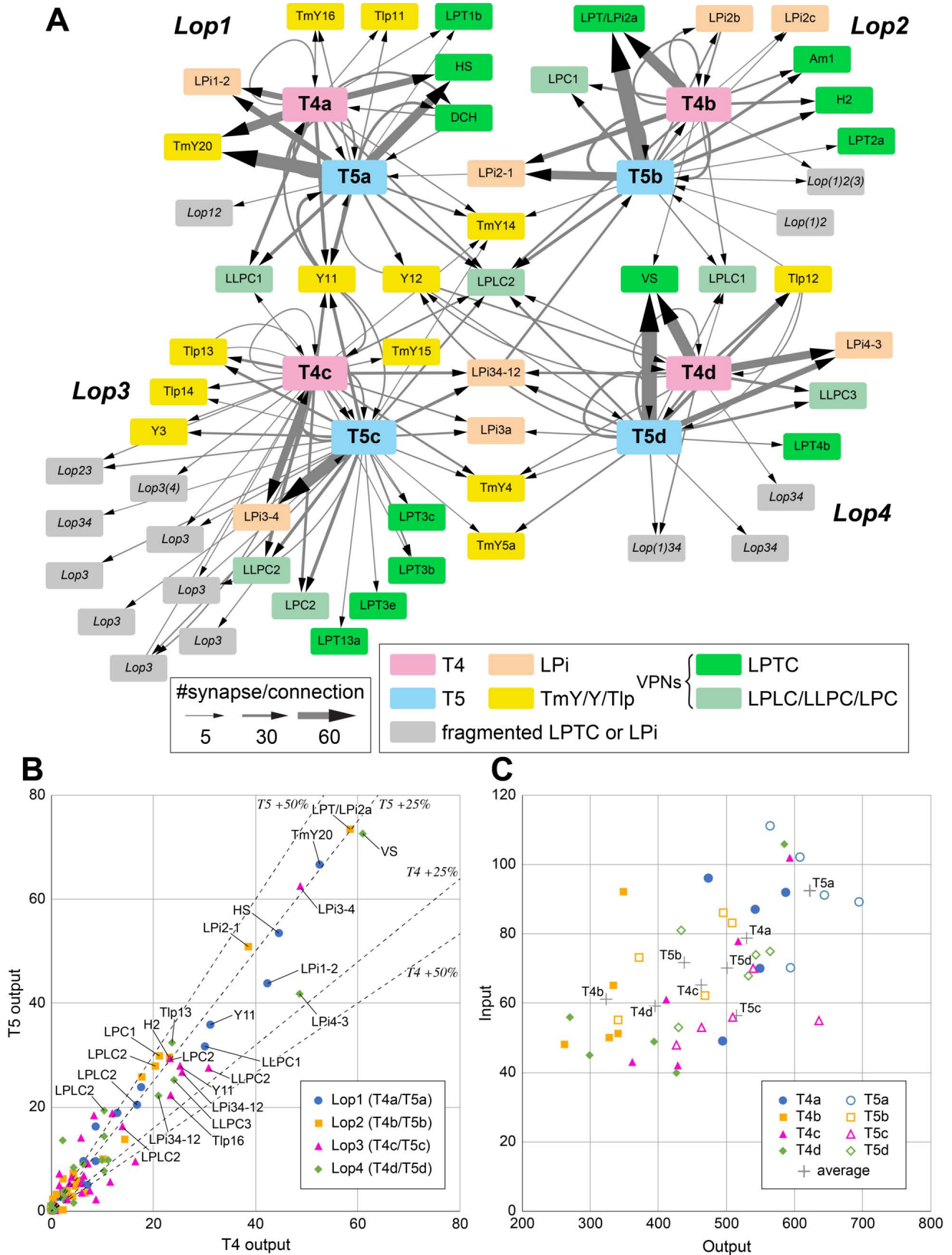


## Figure 2. Connectivity of the seed T4 and T5 cells in the lobula plate.

(A) The inputs and outputs of representative T4 and T5 cells (five cells per each subtype; see text for details, also File S1) in the lobula plate were comprehensively identified. The input and output cells were grouped by the cell type, and inputs and outputs corresponding to a mean of more than five synapses per T4 or T5 cell are shown in the diagram. The thickness of the arrows indicates the average number of synapses per T4 or T5 cell. Each rectangle indicates a cell type; colored rectangles correspond to uniquely identified cells, and gray rectangles represent neurons we could not uniquely identify due to incomplete reconstruction. For unidentified neurons, the main innervated layers are shown in italic letters. For example, *Lop(1)34* means that the fragment has major arbors in Lop3 and Lop4, and minor arbors in Lop1. LPi are lobula plate intrinsic cells, the TmY/Y/Tlp neurons connect the optic lobe neuropils, and LPTC and LPLC/LLPC/LPC cells are visual projection neurons (VPNs) that send outputs to the central brain. (B) Average numbers of output synapses from single T4 and T5 per postsynaptic cell type. Neurons are color-coded by the layer where they receive inputs from T4 and T5. Generally, outputs from T4 and T5 (and therefore inputs to their target neurons) are approximately evenly integrated by the postsynaptic cells, with a slight bias for T5. All named neurons receiving more than an average of 20 synapses from both T4 and T5 are labeled (LPLC2 is labeled for all four layers). The dashed lines indicate 25% and 50% difference from equal numbers of output from T4 and T5 to any target cell type. (C) Total numbers of input and output synapses of the representative T4 and T5 cells. Autapses (self-synapses) and synaptic contacts with glia are excluded from this quantification. Averaged synapse numbers of each cell type (five individual neurons per each cell type) are indicated as gray crosses.



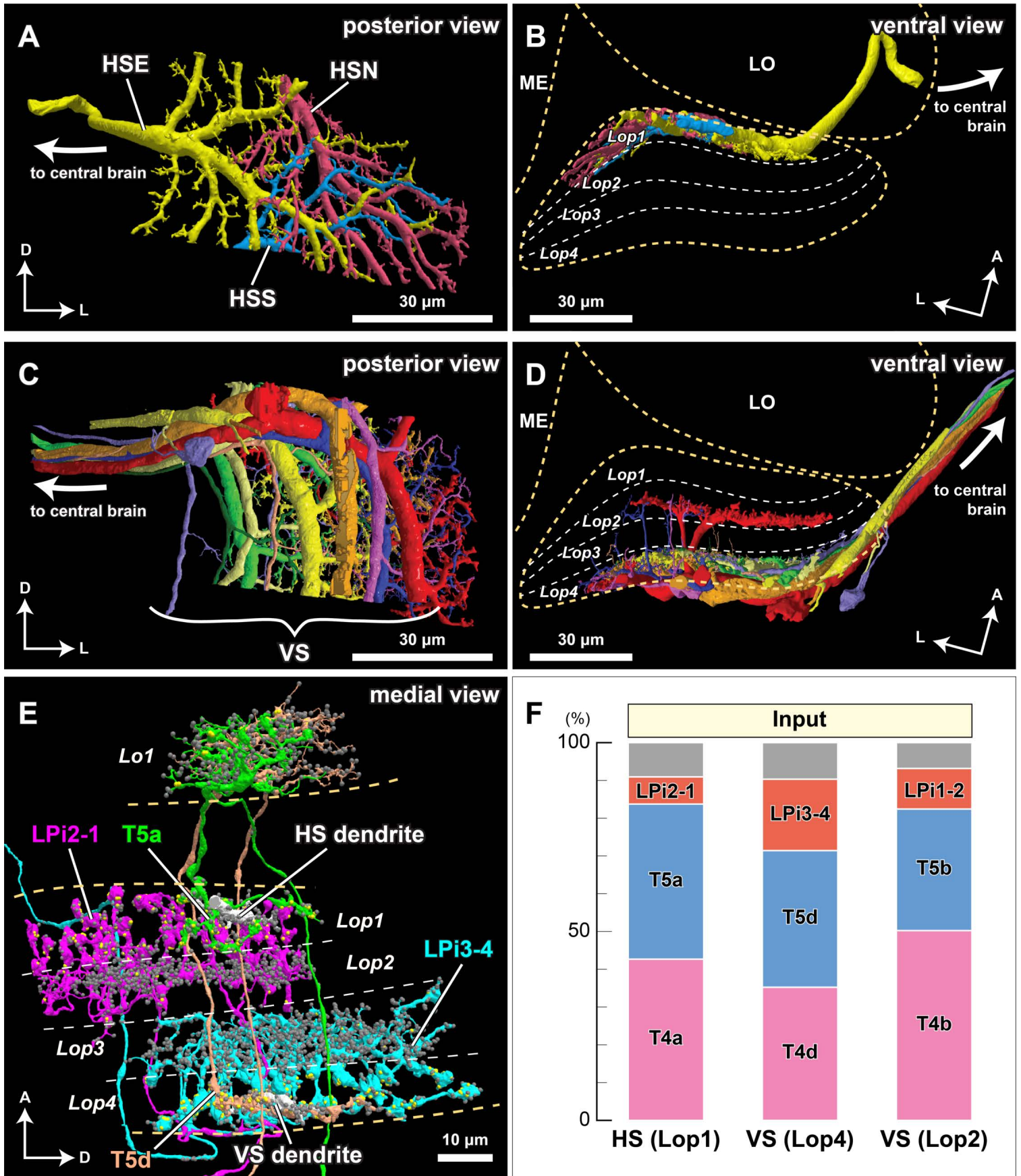


### **Figure 3. Synaptic connections of the horizontal system (HS) and vertical system (VS) lobula plate tangential cells.**

(A, B) The three HS cells (HSN, HSE, and HSS) occupy Lop1, the first layer of the lobula plate. Collectively the dendrites of these neurons span Lop1 and overlap in the region of the lobula plate within our data volume, but are cut off at the edges of the volume. (A) posterior view, (B) ventral view. (C, D) The ten identified VS cells in our data volume. All have postsynaptic terminals in Lop4, while four of them also have branches in Lop2. (C) posterior view, (D) ventral view. (E) Examples of major input neurons to the HS and VS cells in the lobula plate. Single dendritic arbors (length  $\sim 20 \mu\text{m}$ ) of one HS cell and one VS cell are shown in white. HS dendrites primarily receive input from the T4a, T5a, and LPi2-1 cells in Lop1, whereas VS dendrites in Lop4 primarily receive input from the T4d, T5d, and LPi3-4 cells. The T4 terminals are not shown to minimize clutter. Yellow and gray dots represent pre- and postsynaptic sites, respectively. (F) Inputs to the HS and VS cells. Synapses are verified and counted for small pieces of the HS and VS arbors in the respective layers (two branches for each of HS and VS (Lop4) and one branch for VS (Lop2)). Almost 90% of the inputs to the HS and VS cell dendrites come from T4, T5, and the bilayer LPi cells. A similar input distribution is found for the VS cells' branches in the Lop2 layer, where they receive inputs from the T4b, T5b, and LPi1-2 cells. Gray indicates other, more weakly connected neurons or unidentified neuron fragments, less than 10% of the total synapses (detailed in File S2). No output synapses were found on these branches. The scale bars are approximate as the neurons are three-dimensionally reconstructed.

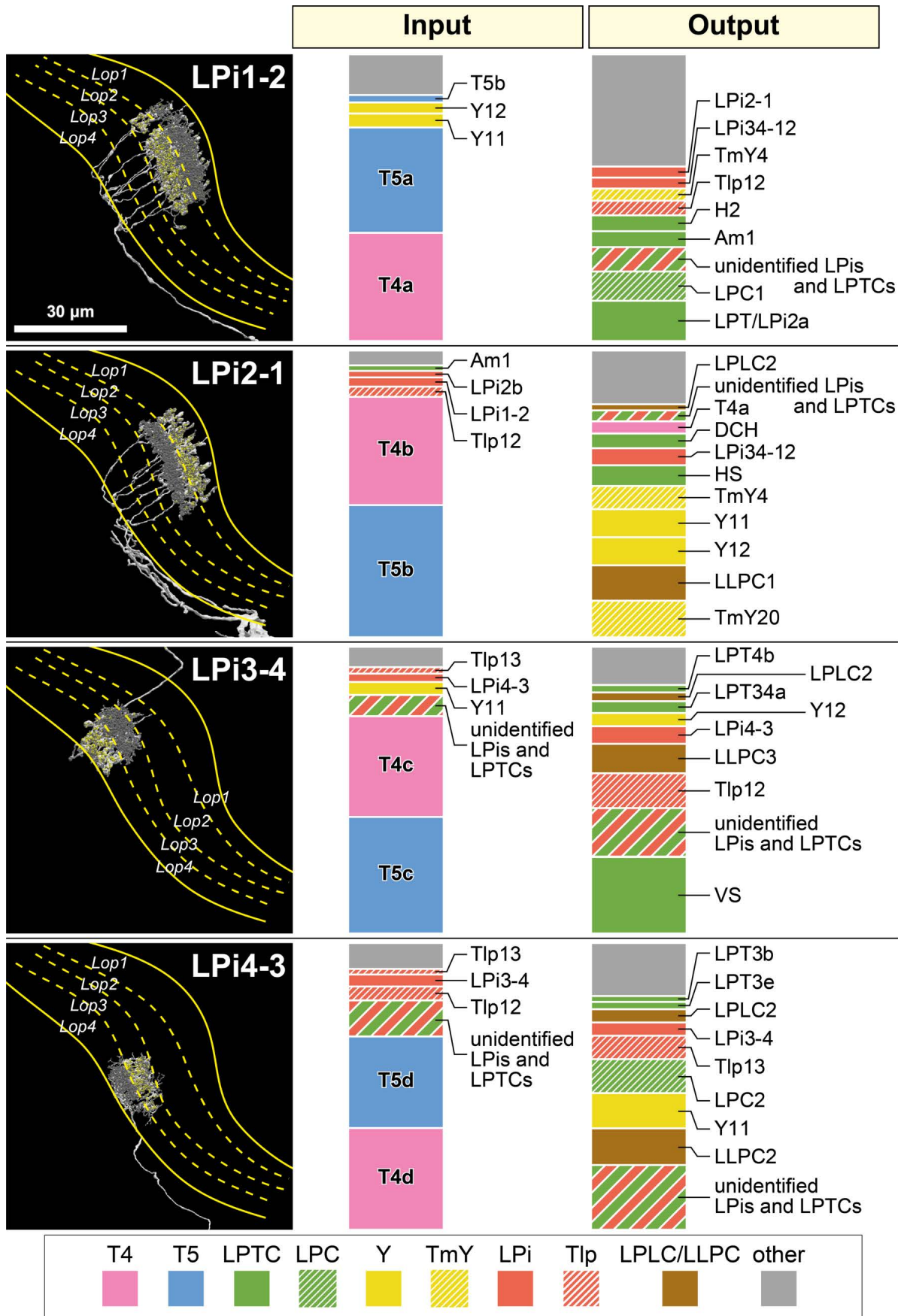


#### **Figure 4. Connectivity of the bilayer Lobula Plate intrinsic (LPi) cells.**

A representative cell of each neuron type is shown in the left panel. Presynaptic sites are indicated with yellow dots and postsynaptic sites are shown with gray dots. These neurons primarily integrate inputs in one layer and supply outputs to the adjacent layer. Only the LPi3-4 cell is completely reconstructed, while the other cells are only partially reconstructed, since single neurons cover larger LOP areas than the imaged data volume. A candidate light microscopy match for LPi1-2 (Figure S1) suggests the possibility that the LPi1-2 reconstructions (and perhaps also the similar LPi1-2 fragments) may be parts of one or a few large cells. In the right two panels, ratios of the input and output synapses are shown for each indicated cell type. These data are based on a single selected branch for each cell type (with 600-1000 postsynaptic sites, 100-170 presynaptic sites), for which the pre- and postsynaptic connected neurons were identified wherever possible. Cell types occupying less than 2% of the total input or output synapses are not shown and are included as “other”. A number of tangential elements that have synapses with the LPi cells were only partially reconstructed due to the restricted data volume. These fragments of considerable size are grouped as “unidentified LPis and LPTCs”. Data summary based on File S3.

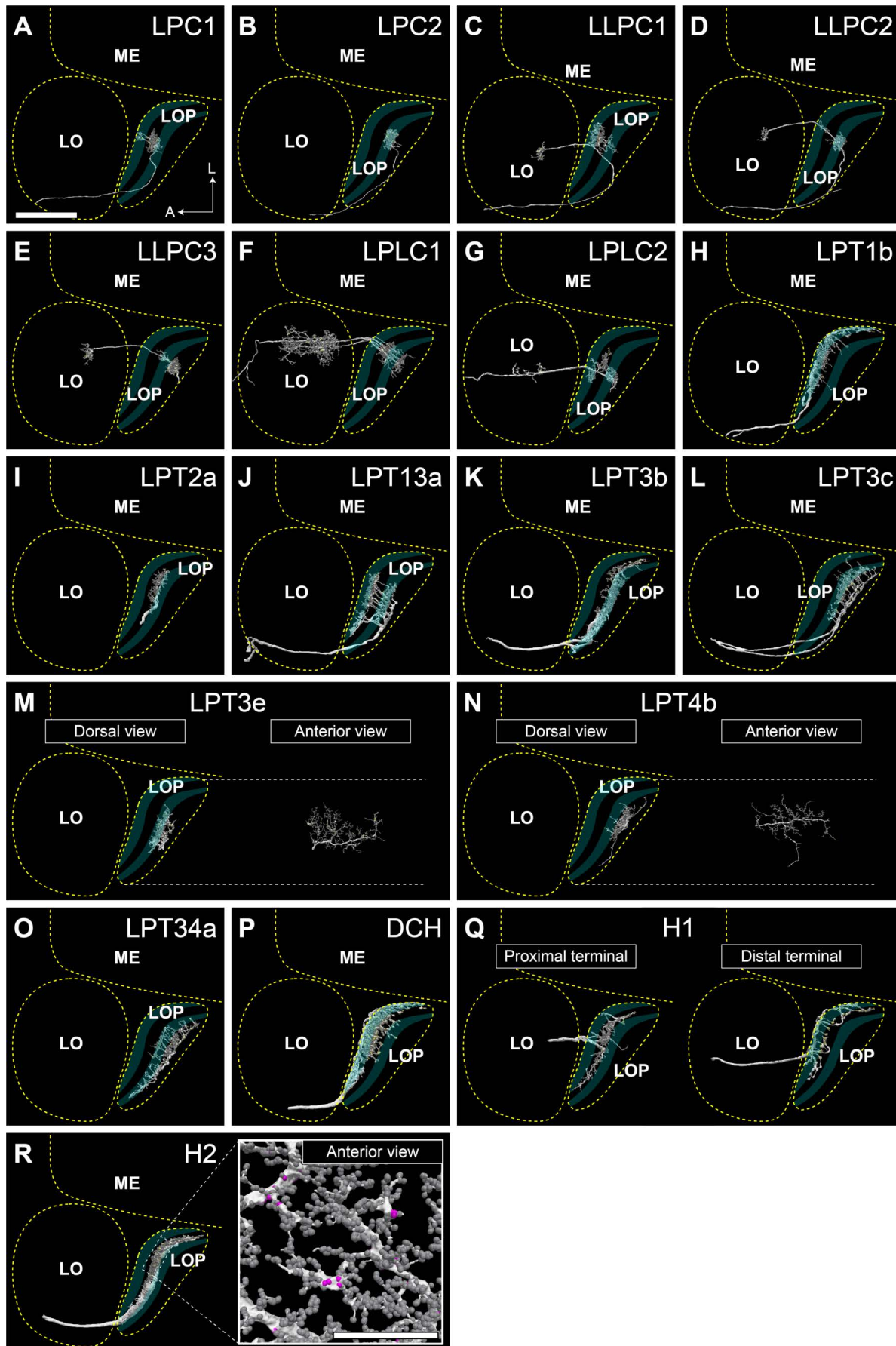


**Figure 5. Lobula plate Visual Projection Neurons (VPNs) that integrate T4 and T5 inputs.**

The neurons are seen from the dorsal direction (horizontal projection), the approximate neuropil boundaries are outlined, and the LOP layers are indicated. Only neurons mentioned in other figures or in the main text are shown here. Some neurons are not fully reconstructed, especially the cell body fibers and the main axons projecting to the central brain. Lobula plate-lobula columnar (LPLC) cells have cell bodies in the cell body ring between the optic lobe and central brain and dendritic arbors in the lobula that extend into the lobula plate<sup>38,40</sup>, and project to the central brain from the lobula. Lobula plate columnar (LPC) and lobula-lobula plate columnar (LLPC) cells have cell bodies in the cell body ring of the lobula plate<sup>38,40,41,43,44</sup>, and project axons along a path posterior to the lobula plate to glomeruli in the posterior lateral protocerebrum. Both LPC and LLPC send a branch into the lobula plate which, in the case of LLPC cells, further extends into the lobula. HS and VS cells are omitted from this figure (see Figure 3). In (R), the branching pattern and synapse distribution is shown in the inset. Pre- and postsynapses are shown in magenta and gray, respectively. In (A), A: anterior, L: lateral. Scale bar: (A-S) 30 $\mu$ m, (R) inset 20 $\mu$ m.

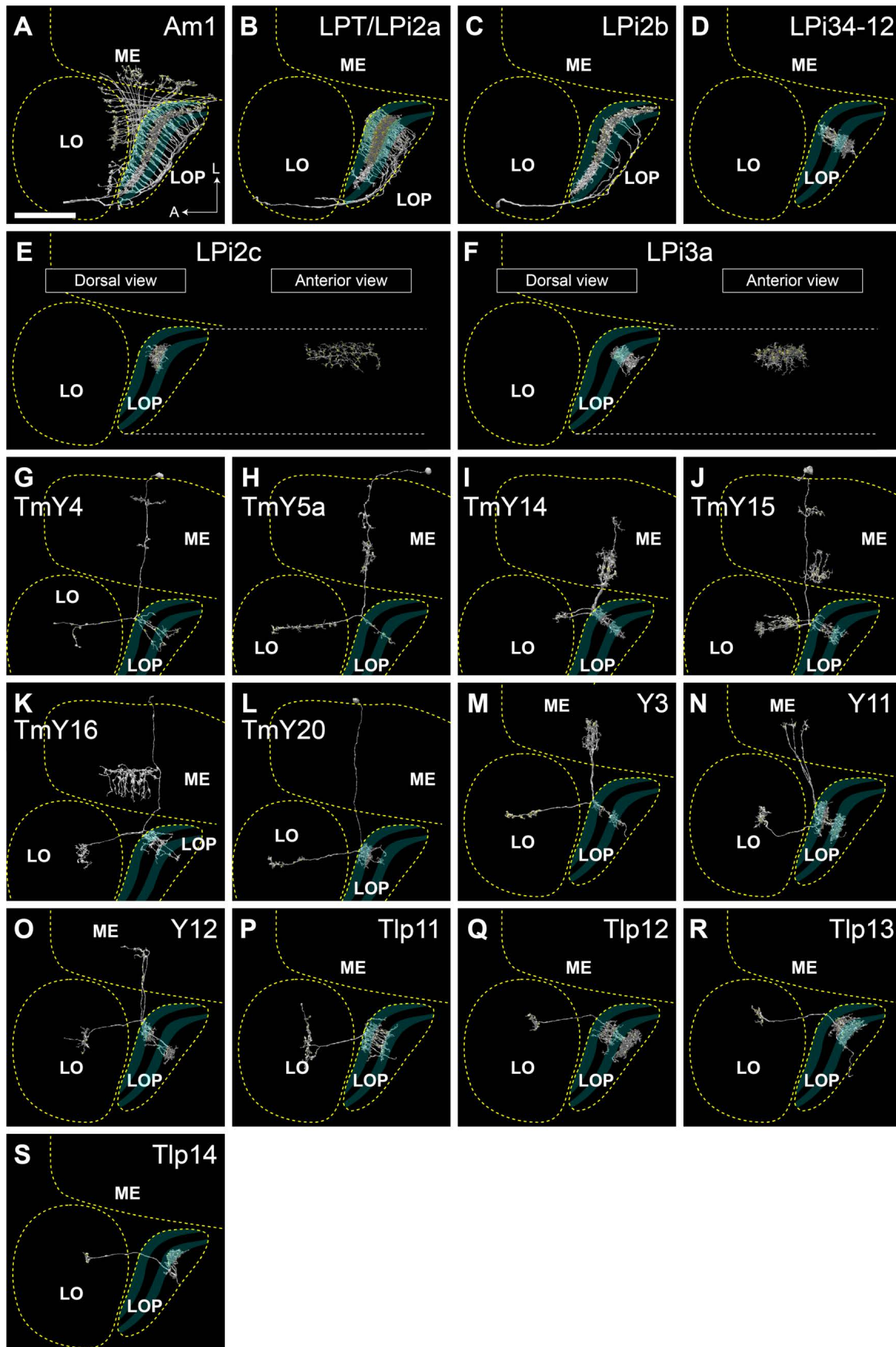


### **Figure 6. Optic lobe intrinsic neurons that integrate T4 and T5 inputs.**

The neurons are seen from the dorsal direction (horizontal projection), the approximate neuropil boundaries are outlined, and the LOP layers are indicated. Only neurons mentioned in other figures or in the main text are shown here. Some of the neurons are not fully reconstructed, especially the cell body fibers. We confirmed the general cell shapes of all newly identified cell types shown in this figure (with the exception of the comparatively small LPi2c and LPi3a fragments) by comparison to light microscopy images (Figures S1 and S2). Based on these matches, LPT/LPi2a may be a type of VPN with a central brain projection. Pre- and postsynapses are shown in magenta and gray, respectively. Scale bar: 30 $\mu$ m.



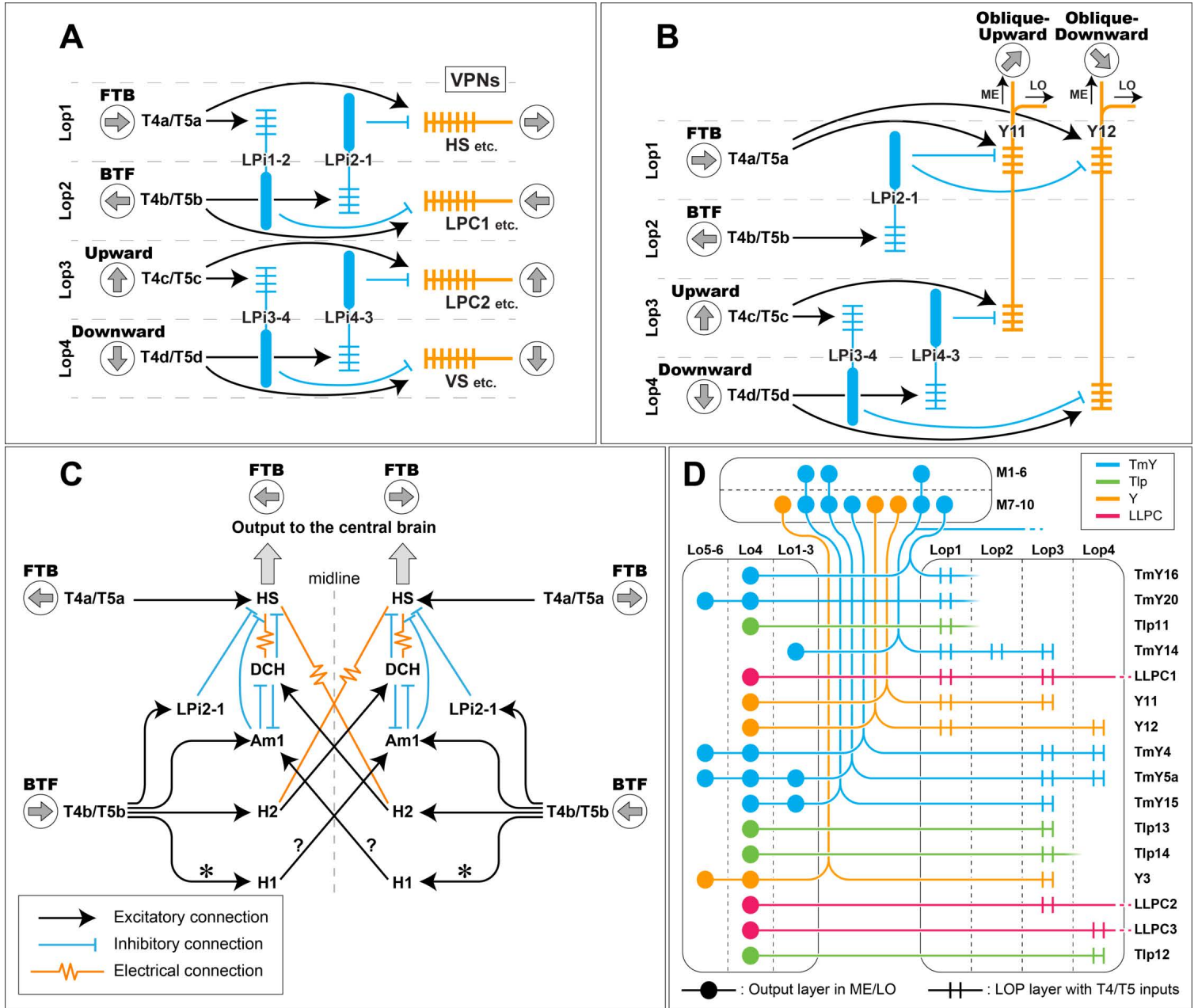


## **Figure 7. Summary of the motion pathway circuitry revealed by the lobula plate reconstruction.**

(A) The primary connections between the T4/T5 cells, bilayer LPi cells, and output VPNs. FTB: front-to-back, BTF: back-to-front. The LPi cells, indicated in blue, are likely all inhibitory cells (based on <sup>35</sup>). Each layer has VPN outputs that are predicted (or known for the few supported by functional studies) to encode motion with the same directional selectivity as the T4/T5 subtypes in that layer. Some VPNs, like the VS cells of Figure 3, integrate inputs from multiple T4/T5 subtypes in different layers. (B) The Y11 and Y12 cells and their LOP inputs. The two Y cell types receive excitatory inputs from T4 and T5 in two layers and (putative) inhibitory inputs from T4 and T5 neurons in the other layers, via bilayer LPi cells. By integrating these inputs, it is expected that these neurons become most sensitive to the direction of overlapping sensitivity of their inputs, and thus Y11's preferred direction would be for oblique-upward motion and Y12 would prefer oblique-downward motion. (C) The bilateral circuitry comprised of horizontal-motion sensitive neurons, including H1, H2, DCH, and Am1 cells, integrating motion from both eyes. Connections within the optic lobe are based on the observation of this dataset, while contralateral projections and synaptic contacts in the central brain are also based on prior studies and datasets, including <sup>43,59,61</sup>. Connections from T4b/T5b to H1, indicated with asterisks (\*), are not shown in Figure 2A, as the synapse numbers per representative were below the threshold, but shown in this diagram since the main inputs to H1 are T4b and T5b. H1 is considered to be a glutamatergic cell <sup>55</sup>, and it is not known whether the signal from H1 is excitatory or inhibitory (see the main text for the detail). Since electrical synapses cannot be directly observed in the FIB-SEM dataset, the indicated connections are based on physical proximity of the axons of these cells in this dataset. The diagrams do not exhaustively list inputs and outputs of the shown neurons. (D) Neurons relaying T4/T5 outputs to the lobula. The paired parallel lines indicate T4/T5 inputs in the lobula plate, whereas the dots represent locations of the output (presynaptic) terminals in the lobula and the medulla. Input (postsynaptic) terminals in the lobula and the medulla, as well as terminals not coupled with T4/T5 in the lobula plate, are omitted. The central brain projections of TmY14 and the LLPC cells are shown as broken lines.

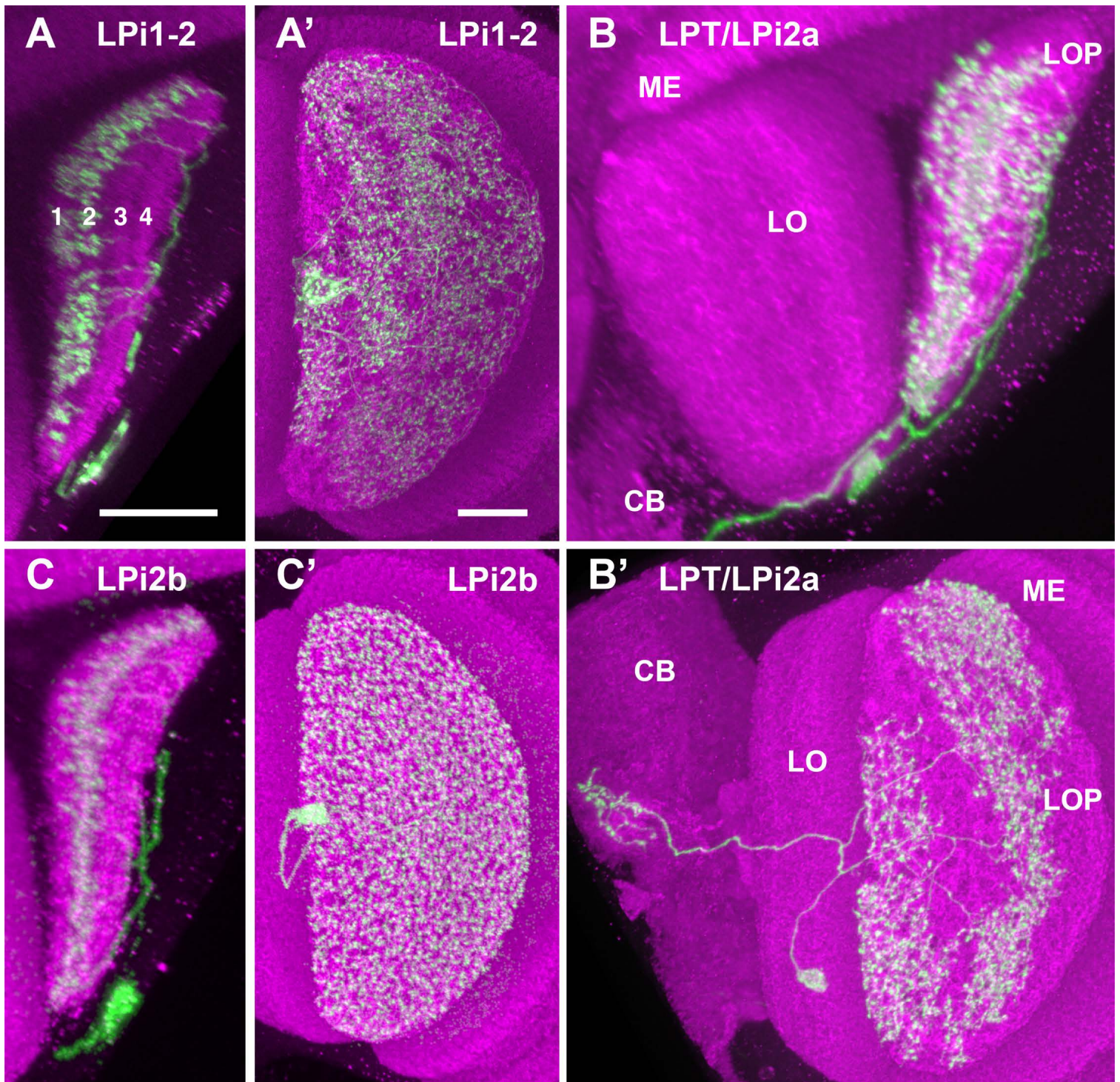


### Figure S1. Candidate light microscopy matches for large LPi-like cells. Related to Figure 6.

Images show resampled views generated from confocal stacks with MCFO-labeled neurons using VVD viewer (see Methods). Some images were manually edited in VVD viewer in order to only show the cells of interest. Panels show either the lobula plate layers (in a view similar to Figures 5 and 6) (A, B, C) or an *en face* view of the lobula plate from posterior (A', B' C'). Cell type names indicate apparent EM matches. Scale bars in A and A' represent 20  $\mu\text{m}$ . Other panels are shown at similar but not identical scale. Note that the neuropils appear to be much smaller than those in the EM sample (e.g., Figure 1A) due to shrinkage from dehydration for DPX mounting (see Methods and also Figure 19 of Scheffer et al. <sup>43</sup>). Numbers in panel A mark lobula plate layers. Brains regions are indicated in (B, B') (CB, central brain).

(A) A large lobula plate intrinsic cell that locally matches the arbor structure (thin processes, likely dendritic in LOP1, varicosities, likely presynaptic, in LOP2; parallel processes to and soma in the lobula plate cell body rind) of LPi1-2 (Figure 4). A') Arbor spread of the neuron in (A). Processes cover most of the LOP in a non-uniform pattern. (B) Layer pattern and lobula plate coverage (B') of a neuron resembling LPT/LPi2a (Figure 6B). Central projection suggests that the neuron we identify in the EM volume as LPT/LPi2a is likely a VPN. (C) Layer pattern of an apparent LM match of LPi2b (Figure 6C). This cell covers all of the lobula plate (C').

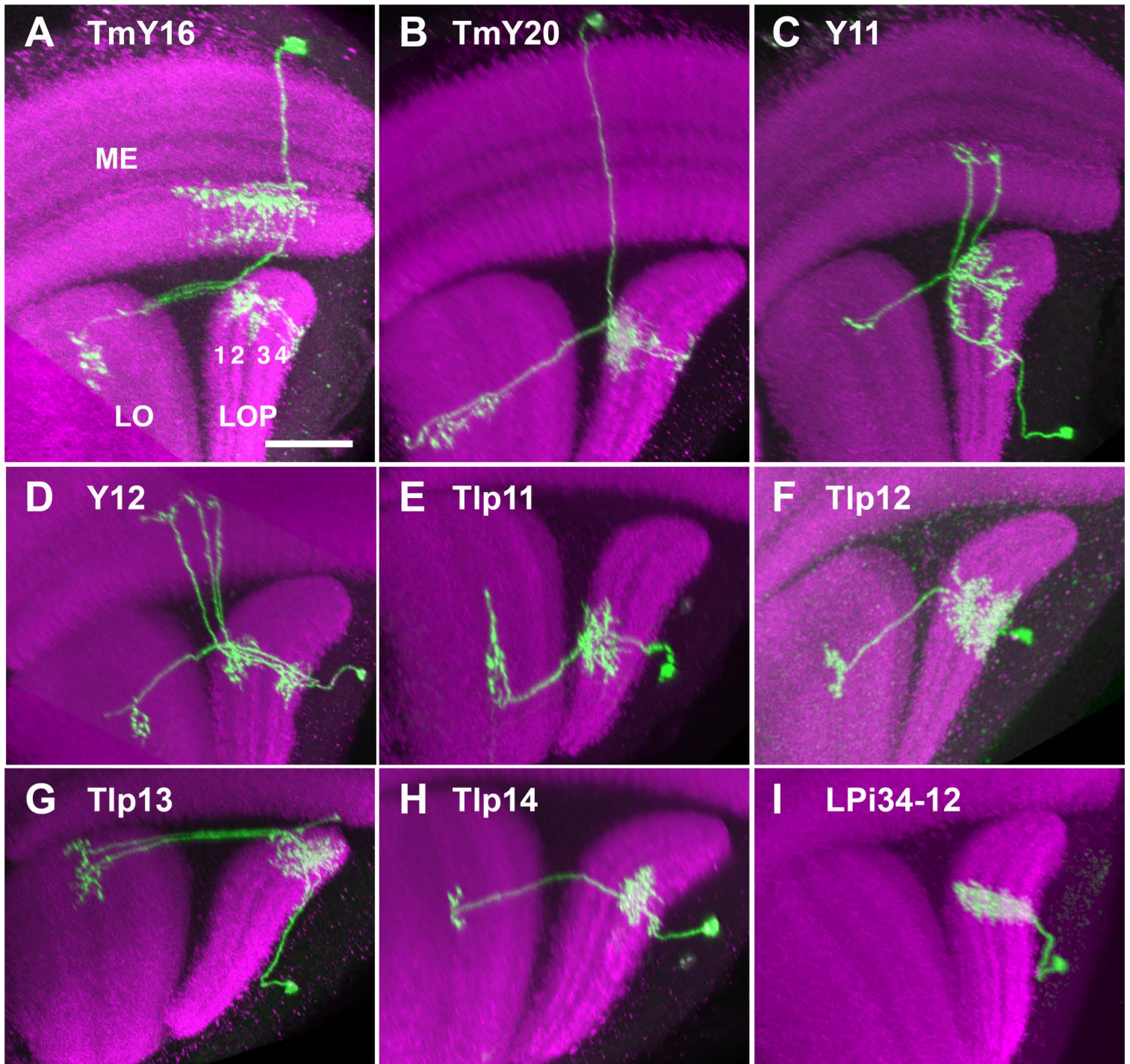


**Figure S2. Candidate light microscopy matches for newly described optic lobe intrinsic cell types. Related to Figure 6.**

Images show resampled views generated from confocal stacks with MCFO-labeled neurons using VVD viewer (see Methods). Some images were manually edited in VVD viewer in order to only show the cells of interest. Panels show the lobula plate layers (displayed in a view similar to Figures 5 and 6). Cell type names indicate apparent EM matches. Scale bar in A represent 20  $\mu\text{m}$ . Other panels are shown at similar but not identical scale. Numbers in panel A mark lobula plate layers, optic lobe regions as indicated. (A) TmY16, (B) TmY20, (C) Y11, (D) Y12, (E) Tlp11, (F) Tlp12, (G) Tlp13, (H) Tlp14, (I) LPi34-12.

## Supplemental Information

**Table S1: Fly crosses used to visualize lobula plate neurons in this study**

Figure panel(s)	Fly cross
S1A, S1A'	R20F11-GAL4 crossed to MCFO-7 (Nern et al 2015)
S1B, S1B'	R15D05-Gal4 crossed to MCFO-7
S1C, S1C'	R42B05-GAL4 crossed to MCFO-7
S2A, S2C, S2D, S2I	OL-KD (29C07-KDGeneswitch-4) in attP40; R57C10-GAL4 in attP2 tubP-KDRT>GAL80- 6-KDRT> in VK00027 crossed to MCFO-1 (Nern et al 2015)
S2B	VT048842-GAL4 crossed to MCFO-7
S2E	R10E08-GAL4 crossed to MCFO-7
S2F	R87B02-GAL4 crossed to MCFO-7
S2G	VT016795-GAL4 crossed to MCFO-7
S2H	VT016279-GAL4 crossed to MCFO-7

### Movie S1. (MovieS1.avi)

#### Rotating movie of the VS, T4d, T5d, and LPi3-4 cells. Related to Figure 3.

VS: magenta, VS dendrite: green, T4d: shades of green, T5d: shades of blue, LPi3-4: red and orange, presynapse: yellow, postsynapse: white.

#### File S1. Connections of the T4 and T5 cells. Related to Figure 2A.

**S1A:** List of input neurons and numbers of synapses of the core T4 and T5 neurons (20 cells each)

**S1B:** List of output neurons and numbers of synapses of the core T4 and T5 neurons (20 cells each)

#### File S2. Outputs of the HS and VS branches. Related to Figure 3F.

**S2A:** List of input neurons and numbers of synapses of HS cell branches

**S2B:** List of input neurons and numbers of synapses of VS cell branches in Lop2

**S2C:** List of input neurons and numbers of synapses of VS cell branches in Lop4

**File S3. Connections of the bilayer LPi cells. Related to Figure 4.**

**S3A:** List of input neurons and numbers of synapses of an LPi1-2 cell branch

**S3B:** List of output neurons and numbers of synapses of an LPi1-2 cell branch

**S3C:** List of input neurons and numbers of synapses of an LPi2-1 cell branch

**S3D:** List of output neurons and numbers of synapses of an LPi2-1 cell branch

**S3E:** List of input neurons and numbers of synapses of an LPi3-4 cell branch

**S3F:** List of output neurons and numbers of synapses of an LPi3-4 cell branch

**S3G:** List of input neurons and numbers of synapses of an LPi4-3 cell branch

**S3H:** List of output neurons and numbers of synapses of an LPi4-3 cell branch